Research

Evaluating the Effect of Gestational Exposure to Perfluorohexane Sulfonate on Placental Development in Mice Combining Alternative Splicing and Gene Expression Analyses

Yihao Zhang,[1,2]* Jia Lv,[1,2]* Yi-Jun Fan,[1,2,3]* Lin Tao,[1,2] Jingjing Xu,[1,2] Weitian Tang,[1,2] Nan Sun,[1,2] Ling-Li Zhao,[1,2] De-Xiang Xu,[1,2,4] and Yichao Huang[1,2,4]

[1]Department of Toxicology, School of Public Health, Anhui Medical University, Hefei, China
[2]Key Laboratory of Environmental Toxicology of Anhui Higher Education Institutes, Anhui Medical University, Hefei, China
[3]Department of Gynecology and Obstetrics, Second Affiliated Hospital, Anhui Medical University, Hefei, China
[4]Key Laboratory of Population Health Across Life Cycle, Anhui Medical University, Ministry of Education of the PRC, Hefei, China

BACKGROUND: Perfluorohexane sulfonate (PFHxS) is a frequently detected per- and polyfluoroalkyl substance in most populations, including in individuals who are pregnant, a period critical for early life development. Despite epidemiological evidence of exposure, developmental toxicity, particularly at realistic human exposures, remains understudied.

OBJECTIVES: We evaluated the effect of gestational exposure to human-relevant body burden of PFHxS on fetal and placental development and explored mechanisms of action combining alternative splicing (AS) and gene expression (GE) analyses.

METHODS: Pregnant ICR mice were exposed to 0, 0.03, and 0.3 μg/kg/day from gestational day 7 to day 17 via oral gavage. Upon euthanasia, PFHxS distribution was measured using liquid chromatography-tandem mass spectrometry. Maternal and fetal phenotypes were recorded, and histopathology was examined for placenta impairment. Multiomics was adopted by combining AS and GE analyses to unveil disruptions in mRNA quality and quantity. The key metabolite transporters were validated by quantitative real-time PCR (qRT-PCR) for quantification and three-dimensional (3D) structural simulation by AlphaFold2. Targeted metabolomics based on liquid chromatography–tandem mass spectrometry was used to detect amino acid and amides levels in the placenta.

RESULTS: Pups developmentally exposed to PFHxS exhibited signs of intrauterine growth restriction (IUGR), characterized by smaller fetal weight and body length ($p < 0.01$) compared to control mice. PFHxS concentration in maternal plasma was 5.01 ± 0.54 ng/mL. PFHxS trans-placenta distribution suggested dose-dependent transfer through placental barrier. Histopathology of placenta of exposed dams showed placental dysplasia, manifested with an attenuated labyrinthine layer area and deescalated blood sinus counts and placental vascular development index marker CD34. Combined GE and AS analyses pinpointed differences in genes associated with key biological processes of placental development, proliferation, metabolism, and transport in placenta of exposed dams compared to that of control dams. Further detection of placental key transporter gene expression, protein structure simulation, and amino acid and amide metabolites levels suggested that PFHxS exposure during pregnancy led to impairment of placental amino acid transportation.

DISCUSSION: The findings from this study suggest that exposure to human-relevant very-low-dose PFHxS during pregnancy in mice caused IUGR, likely via downregulating of placental amino acid transporters, thereby impairing placental amino acid transportation, resulting in impairment of placental development. Our findings confirm epidemiological findings and call for future attention on the health risk of this persistent yet ubiquitous chemical in the early developmental stage and provide a new approach for understanding gene expression from both quantitative and qualitative omics approaches in toxicological studies. https://doi.org/10.1289/EHP13217

Introduction

Per- and polyfluoroalkyl substances (PFAS) are a large group of fluorine-containing chemicals commonly applied in industrial and commercial products, resulting in ubiquitous presence in the environment[1,2] and attracting significant attention. These chemicals are also named "forever chemicals," due to their high chemical stability and bioaccumulation in the environment.[3] Two of the most commonly reported PFAS congeners perfluorooctanoic acid (PFOA)

and perfluorooctane sulfonate (PFOS) were listed in the Stockholm Convention in 2019,[4] due to substantial research attention on their toxicities and advocacy from public health scientists and environmental agencies. Hence, the use of substitute chemicals has expanded substantially thereafter, leading to the total number of PFAS chemicals reaching $> 1,400$.[3] Among these PFAS alternatives, perfluorohexane sulfonate (PFHxS) is one of the most frequently reported chemicals with respect to its environmental occurrence.[5–7]

Increasing evidence has confirmed widespread human exposure to PFHxS, the third most-abundant PFAS in most populations including during pregnancy, a period deemed critical for early life development.[8–11] Entering the body mainly via oral ingestion,[12,13] gestational exposure to PFHxS have been suggested to be associated with adverse health consequences on the expectant mothers and fetuses in mice[14] and humans.[15] Epidemiological studies demonstrated that exposure to PFAS during pregnancy was linked to lower birth weight,[16,17] preeclampsia,[18] and pregnancy-induced hypertension.[19] These associated adverse health consequences in relation to PFAS exposure may exert longer-lasting health effects in later childhood.[20–22] Following the increasing body of evidence from human studies, PFHxS was recently added in the Stockholm Convention list as a chemical of emerging concern.[23] Despite the abundance of human epidemiological evidence on the associations between gestational exposure and birth outcomes, the developmental effects of the chemical PFHxS on fetal development, particularly at realistic human exposures, remain to be confirmed in experimental models along with the underlying mechanisms.

The placenta is an important organ linking the mother to the fetus, supplying oxygen and nutrients to the developing fetus. Ample recent literature demonstrated that PFAS chemicals including PFHxS could cross the maternal-fetal barrier and bioaccumulate in the placenta and the fetus via umbilical cord blood in pregnant women[8–11,24] and CD-1 pregnant mice.[25] It was speculated that the detection of these chemicals might be associated with compromised bioactivity of transporter proteins in the placenta using computational studies,[26] hence explaining the potential relationship to developmental abnormalities. These human observational association studies and computational docking studies, however, do not provide a direct causal explanation for the developmental toxicities of PFHxS, hence requiring animal mechanistic studies. To the best of our knowledge, no data have been reported to demonstrate the potential developmental toxicity of PFHxS at human-relevant body burden doses.

Thus, the objectives of the current study were to investigate gestational exposure of mice to human-relevant doses (0.03 and 0.3 µg/kg/day) of PFHxS, orders of magnitude lower than PFOS (2.5 mg/kg/day, a dose which decreased placenta size and fetal weight[27]) or PFOA (5 mg/kg/day, a dose which impaired follicle development in mice[28]), and its toxic effect on fetal development as well as the potential toxicological mechanisms underlying placenta impairment in mice. We have, to our knowledge, for the first time combined alternative splicing and genome-wide expression analyses to comprehensively evaluate integrity and quantity of mRNAs that are essential in placental function and fetal development. Our work will provide key data for the developmental toxicity of PFHxS upon *in utero* exposure at human-relevant very low doses, provide direct evidence for epidemiological findings regarding its associations with lower birth weight using a new multiomics approach, and may question the suitability of this substitute chemical to PFOS or PFOA.

Materials and Methods

Animals

Eight-week-old specific-pathogen-free (SPF) ICR adult animals (male and female) were purchased from Beijing Vital River Laboratory Animal Technology Co., Ltd (Beijing, China). Animals were raised in an SPF-grade animal room with a 12-h light/dark cycle and provided with food and water *ad libitum*. Experimental animals were fed with growth and reproduction compound feed, which was purchased from Keao Xieli Feed Co., Ltd (Beijing, China). All experimental procedures were carried out in accordance with the regulations of the Anhui Medical University Animal Care and Use Committee and Use of Laboratory Animals (LLSC20211179, Hefei, China). Experimental animals were mated at a ratio of 2:1 (female: male). Pregnant mice were randomly divided into three groups as follows: control [corn oil (Aladdin, China; C116025) with 0.03% dimethylsulfoxide (DMSO) (MedChemExpress, USA; HY-Y0320, CAS No. 67-68-5; ≥99.0%)] or 0.03 or 0.3 µg/kg body weight/day PFHxS (Macklin, China; P850157, CAS No. 355-46-4; ≥95%) in 0.03% DMSO in corn oil with six animals in every group. Vaginal plug was observed to confirm successful mating. During gestational day (GD) 7 to GD17, PFHxS was administered by oral gavage at 3 µL/g body weight once a day containing varying concentrations of the chemical. Pregnant mice were gently handled, and general information of experimental mice including body weight and food consumption were weighed daily in the morning.

The selection of the dosage range was based on the tolerable daily intakes (TDI) of PFOS at 150 ng/kg of body weight set by the European Food Safety Authority.[29] To account for variations in dose-responses among humans (a correction factor of 10×),[30] the exposure dose of animals was calculated to be 1.5 µg/kg/day.

Considering some other confounding factors and variables, an equivalent dose of 0.3 µg/kg/day was defined. To further confirm the validity of our internal exposure dose, we consulted the human biomonitoring of PFAS in German blood plasma samples from 1982 to 2019, demonstrating that the level of PFHxS in human plasma was in a range of <limit of quantitation (LOQ) to 4.62 ng/mL.[6] In our study, it was 4.34–5.46 ng/mL in maternal blood in the high-dose group (0.3 µg/kg/day group) in Figure 1C, which was relevant to the real human exposure burden.

At GD18, pregnant mice were euthanized with pentobarbital sodium. And fetal weight, fetal body length, placenta weight and placenta diameter were each recorded by the same technician to minimize variation. Maternal blood, placenta, and fetal serum were collected for subsequent experiments. The experimental design was shown in Figure 1A.

Hematoxylin-Eosin Staining

Fresh placental tissue was soaked in 4% paraformaldehyde and fixed in a shaking table at room temperature for 24 h. The fixed tissues were dehydrated by ethanol gradient and embedded in paraffin wax. Paraffin-embedded placentae sections were cut in 5 µm thickness. The development of labyrinth zone (LZ) and blood sinus were observed by staining tissue sections with hematoxylin and eosin (H&E) according to standard methods. Image ProPlus 6.0 (Media Cybernetics, USA) was used to calculate area. Eight replicate biological samples from each group (4 males and 4 females) were randomly selected for histological statistics of LZ area and blood sinus area. For each film, we took eight microscopic fields (2,000 × 1,800 pixels, covering the whole placental area) under 400× field of view. Then, we counted blood sinus area to indicate the development of LZ in the placenta.
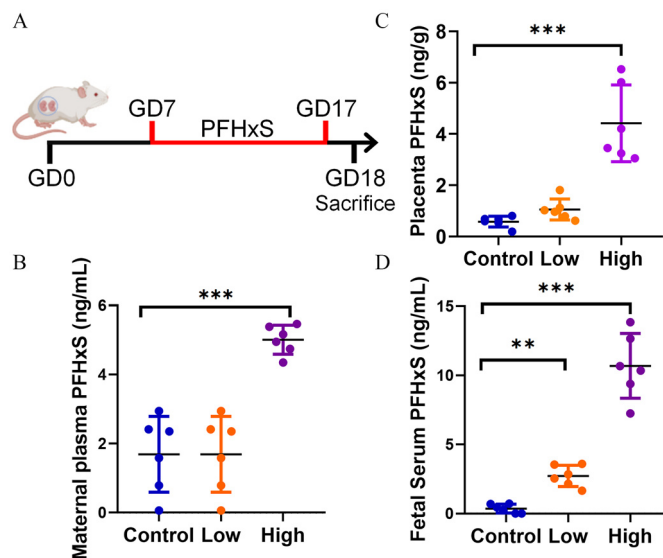

Figure 1. Experimental design scheme and PFHxS distribution across placenta from GD7 to GD17 (mean ± SEM). The exposure doses were 0.3 (high) and 0.03 (low) µg/kg/day, which were administered in corn oil with 0.03% DMSO, and the control was corn oil with 0.03% DMSO. (A) Study design. $n = 6$ litters for each exposure group in the study design. (B) Maternal serum PFHxS at GD18; $n = 6$ dams for each group. (C) Placenta PFHxS at GD18; $n = 6$ for each group, and each data point was obtained by averaging data from one male and one female. (D) Fetal serum PFHxS at GD18; $n = 6$ for each group, and each data point was obtained by the averaging data from one male and one female. p-Values were determined by one-way analysis of variance, [*]$p < 0.05$, [***]$p < 0.001$. Data in panels B–D are also presented in Excel Table S9. Note: DMSO, dimethyl sulfoxide; GD, gestational day; PFHxS, perfluorohexane sulfonate; SEM, standard error of the mean.

Immunohistochemistry

Fresh placental tissue was soaked in 4% paraformaldehyde and fixed in a shaking table at room temperature for 24 h. The fixed tissues were dehydrated by ethanol gradient and embedded in paraffin wax to obtain a 5-μm-thick tissue section. Immunohistochemistry was performed using the rabbit two-step method kit (PV-6001; OriGene, China) according to standard steps. After they were blocked by sheep serum, tissue sections were incubated at 4°C for 20 h in 1:200 CD34 primary antibody (ab81289; Abcam, USA). Then, tissue sections were washed and incubated with an anti-rabbit immunohistochemistry kit (PV-6001; ZSGB-BIO, Beijing, China) according to the manufacturer's protocol at 37°C for 45 min. A fresh brown diaminobenzidine chromogenic kit (ZLI-9019, 20×; OriGene, China) was used for color reaction, and Harris and Mayer hematoxylin was used for reverse staining. Eight replicate biological samples from each group (four males and four females) were selected in each group. For each immunohistochemical film, we took eight microscopic fields ($2,000 \times 1,800$ pixels, covering the whole placental area) under a $400 \times$ field of view by Image Pro Plus 6.0 (Media Cybernetics, USA). Then, we counted the number of CD34-positive blood vessel pairs and calculated the average number of positive blood vessels to indicate the development of blood vessels in placenta.

Determination of PFHxS Concentration

The PFHxS levels of gestational plasma, placenta, and fetal serum were detected by liquid chromatography–tandem mass spectrometry (LC-MS/MS) (AB Sciex 3500, USA) and chromatographic separation using Poroshell 120 EC-C18 (2.1×100 mm, 2.7 μm; Agilent Technologies, USA). The placenta homogenization buffer or plasma/fetal serum (100 μL) was mixed with PFOA internal standards (100 μL). Then, the samples were sonicated 15 min after rapid mixing and extracted with solid-phase extraction cartridges (SPE column, HLB, 1 cc, 30 mg; Waters Corporation, MA, USA). Instrumental information is available in Excel Table S1 and S2. Six biological replicates were measured in each group for maternal blood, placenta, and fetal serum blood, of which each data point for placenta and fetal serum PFHxS concentrations was obtained by averaging data from one male and one female from the same dam.

RNA Sequencing and Data Analysis

Six placentae were included for RNA sequencing in each group, including three males and three females. Total RNA was extracted from placental tissues using the Invitrogen TRIzol Reagent (15596026; Thermo Fisher Scientific, USA) according to the manufacturer's instructions, and RNA quality was assessed by the Agilent 2100 Bioanalyzer and quantified by the NanoDrop 2000 spectrophotometer. RNA integrity number (RIN) values of all samples were >9.0. Reverse transcription of RNA and library construction were performed using TruSeq RNA sample prep kit (FC-122-1001; Illumina, USA) according to the manufacturer's instructions. RNA sequencing was performed using NovaSeq 6000 S2 reagents (20028314; Illumina, USA) on a NovaSeq 6000 system (Illumina, USA) with 150-nucleotide paired-end reads. The cDNA libraries were quantitated by the QuantiFluor double-stranded DNA (dsDNA) system (E2671; Promega, USA). The raw paired-end reads were trimmed and quality controlled by fastp (https://github.com/OpenGene/fastp) with default parameters. The clean reads were separately aligned to reference genome (Mouse Genome Assembly GRCm39) with orientation mode by the HISAT2 version 2.1.0 software (http://ccb.jhu.edu/software/hisat2/index.shtml). The mapped reads were assembled by the StringTie version 2.1.2 software (https://ccb.jhu.edu/software/stringtie/) and followed a genome-guided transcriptome assembly approach along with concepts from de novo genome assembly.[31] One placenta tissue per dam and a total of six biological replicates per group were selected in each group. RNA sequenced raw data are presented in Excel Table S3.

Differentially expressed gene (DEG) analysis was performed using the DESeq2 version 1.40.2 (http://bioconductor.org/packages/release/bioc/html/DESeq2.html)[32] software with a standard of |fold change| ≥ 1 and p-value of <0.05. All alternative splice events that occurred in each sample were identified by using rMATS version 4.1.2 software (http://rnaseq-mats.sourceforge.net/index.html). Only the isoforms that were similar to the reference or comprised novel splice junctions were considered, and the splicing differences were detected in five events, including mutually exclusion exon (MXE), skipped exon (SE), retained intron (RI), alternative 5' splice site (A5SS), and alternative 3' splice site (A3SS). Differentially alternative splice events were identified according to false discovery rate (FDR) <0.05 and |Δ percent spliced-in (ΔPSI)| > 0. Gene ontology (GO), Kyoto Encyclopedia of Genes and Genomes (KEGG), and Reactome analyses were performed using goatools version 1.3.1 (https://pypi.org/project/goatools),[33] KOBAS version 3.0.0 (http://bioinfo.org/kobas/download/),[34] and ReactomePA version 1.44.0 (http://bioconductor.org/packages/release/bioc/html/ReactomePA.html) software,[35] respectively. Gene set enrichment analysis (GSEA) and gene set variation analysis (GSVA) were performed using GSEA version 4.1.0 (https://www.gsea-msigdb.org/gsea/index.jsp)[36,37] and GSVA version 1.46.0 (https://bioconductor.org/packages/3.17/bioc/html/GSVA.html) software.[38] The pathways with p-values <0.05 were considered to be significantly enriched in GO analysis, KEGG analysis, Reactome analysis, and GSVA as well as those with |normalized enrichment score (NES)| > 1 and FDR <0.25 in GSEA.

Quantitative Real-Time PCR Analysis

To validate gene expression levels of amino acid and amides transporters in the animal placenta, the transporter gene expression, including *Slc36a4*, *Slc38a10*, *Slc1a5*, *Slc38a1*, *Slc7a2*, *Slc7a5*, *Slc7a6*, *Slc7a7*, *Slc7a8*, *Slc7a11*, *Slc38a6*, and *Slc16a1* were detected by quantitative real-time PCR (qRT-PCR). The specific gene primers and programs are listed in Excel Table S4. All primers were synthesized from Sangon Biotech (Shanghai, China). The placenta tissues (50 mg) were homogenized in Invitrogen TRIzol Reagent (15596026; Thermo Fisher Scientific, USA), and then total RNA was extracted according to the manufacturer's instructions. Then, reverse transcription of RNA was performed using a Reverse Transcription system (A3500; Promega, USA) to obtain cDNA by Biometra T-Gradient (Biometra biomedizinische Analytik GmbH, Germany). The cDNA library was amplified using the FastStart SYBR Green Master (Roche, Germany; 03003230001) and quantified using the LightCycler 480 II (Roche, Germany). Detailed methods were discussed in a previous study.[39] According to cycle threshold (Ct) values of the samples and primer amplification efficiency (Excel Table S4), the transcript expression levels were analyzed by both the $2^{-\Delta \text{Ct}}$ method and Pfaffl method.

Determination of Amino Acids and Amides in the Placenta

The metabolite levels of amino acids and amides in placenta were determined by LC-MS/MS. About 50 mg of placental tissue was homogenized in cold saline. An aliquot of 200 μL homogenate was taken and added with extraction solvents [acetonitrile (CAS No. 75-05-8, ≥99.9%, 1000291000; Merck, USA) and methanol (CAS No. 67-56-1, ≥99.9%, 1060351000; Merck, USA) 1:1, vol/vol] containing internal standards mixture and vortexed for 5 min. After incubation at $-20°C$ for 2 h and centrifugation for 10 min ($14,000 \times g$, 4°C), the supernatant was transferred and then dried by gentle nitrogen flow. The sample was then reconstituted in 150 μL solvent (acetonitrile and water 1:1, vol/vol) for LC-MS/

MS analysis (AB Sciex 5500, USA). Chromatographic separation was performed on an ACQUITY Premier HSS T3 column (1.8 μm, 2.1 × 150 mm; Waters ACQUITY UPLC, USA) on a binary LC system following previous methods.[40] Detailed methods can be found in Excel Table S5 and Table S6. Quality assurance and quality control procedures included two procedural blanks, two solvent blanks, and a median standard solution for each dozen samples. Ten placenta tissue samples from five litters (each with one male and one female) were measured in each group.

Simulation of Protein 3D Structure

The amino acid sequences and structures of Slc1a5, Slc7a6, and Slc7a7 prototypes were downloaded from the Uniprot database (Release 2023_04; https://www.uniprot.org/),[41] and their DNA sequences were obtained from the University of California Santa Cruz (UCSC) genome database (Release GRCm39; http://genome.ucsc.edu).[42] The DNA sequences of *Slc1a5*, *Slc7a6*, and *Slc7a7* splicing variants were calculated based on the location of alternative splicing (AS) events in the DNA sequence of the prototype (Excel Table S7). The amino acid sequences of Slc1a5, Slc7a6, and Slc7a7 splicing variants were calculated using the Expasy translate tool (https://web.expasy.org/translate/) based on their DNA sequences (Excel Table S8). The obtained amino acid sequences were analyzed and aligned using ESPrint version 3.0.8 tool (https://espript.ibcp.fr)[43] with a global score of 1.0 and gap-between-blocks value of 3. The three-dimensional (3D) structure of Slc1a5, Slc7a6, and Slc7a7 splicing variants were simulated using AlphaFold version 2.3 (https://www.deepmind.com/research/highlighted-research/alphafold) based on the aligned amino acid sequences. Five structural models of each splicing variants were obtained, and each model was repeated three times and optimized using the Amber module within the platform.

Statistical Analysis

All data in this study are described as mean ± standard error of the mean (SEM). After normality tests, the differences between two groups were analyzed by Student's *t* test. One-way analysis of variance was done between treatment groups and control, and if meaningful, further Student's *t* test pairwise comparisons were computed. Statistical analyses and figure illustrations were performed with SPSS 23.0 (SPSS, USA) and GraphPad Prism 8.0 (GraphPad, USA). The *p*-values were determined by hypergeometric test in GO, KEGG, and Reactome pathway enrichment analysis or permutation test in GSEA or Wald test in DEG analysis. FDR values were determined by the Benjamini-Hochberg method. The level of significance was set at $p < 0.05$.

Results

PFHxS Concentration Distribution across Placenta

We exposed pregnant dams to 0, 0.03, and 0.3 μg/kg/day from GD7 to GD17 and measured PFHxS concentration in maternal plasma and placenta and fetal serum among dosed groups to investigate body distribution across the placenta. The results showed that PFHxS was detected in maternal plasma and placenta and fetal serum in both treatment groups. In addition, the measured PFHxS levels were significantly higher in samples from PFHxS-exposed animals, particularly those in the high-dose group, than in control animals ($p < 0.05$) (Figure 1B–D; Excel Table S9). Maternal plasma PFHxS concentration was 5.01 ± 0.54 ng/mL in the high-dose group (0.3 μg/kg/day), which was similar to plasma PFHxS measured in samples collected from 2009 to 2019 as part of the German Environmental Specimen Bank.[6] The higher levels of PFHxS measured in the fetal serum (control: 0.36 ± 0.29 ng/mL;

low-dose: 2.72 ± 0.70 ng/mL; high-dose: 10.69 ± 2.14 ng/mL) suggest that PFHxS traversed the placenta in a dose-dependent manner.

Animal Phenotypes following Gestational Exposure to PFHxS

To evaluate the effect of maternal PFHxS exposure during pregnancy on the development of the fetuses, pregnant mice were exposed to different concentrations of PFHxS from GD7 to GD17. The litters of the high-dose group displayed significantly smaller fetal body length and lower weight compared to the control group in both male and female fetuses (Figure 2A–M; Excel Table S10) at GD18. The body weight, food consumption, liver/body weight ratio, and brain/body weight ratio of gestational mice and live births were not different between dose groups (Figure S1; Excel Table S18).

Placental Development following Gestational Exposure to PFHxS

We further investigated the effect of gestational exposure on the placenta, which is key for fetal growth. Compared with the control group, placenta weight and diameter in the high-dose group was significantly lower (Figure 2D,E; Excel Table S10). We further analyzed placental morphology using H&E staining and interestingly observed that compared with the control group, the percentage of placental LZ was significantly lower in the high-dose group. Moreover, the proportion of blood sinus area in the high-dose group was also significantly lower in both male and female fetuses (Figure 3A–C,F–H; Excel Table S11). In addition, we observed significantly less protein expression of placental vascular development index marker CD34 using immunohistology in both male and female fetuses ($p < 0.01$) (Figure 3D,E,I,J; Excel Table S11).

Gene Expression Analyses of Biological Processes in the Placenta

Next, we investigated the potential underlying mechanism of placental dysplasia associated with 0.3 μg/kg/day PFHxS exposure using an omics screening approach. Transcriptome analysis of placenta was performed using RNA sequencing. As shown in Figure 4A,B (Excel Table S12), the genome-wide expression profiles of the placentae in the high-dose group were significantly different than those in the control group, including 1,104 down-regulated genes and 1,240 up-regulated genes (|fold change| ≥ 1). The role of these DEGs in placental dysplasia was evaluated by GO analysis and GSEA. As displayed in Figure 4C (Excel Table S12), DEGs were enriched in the biological processes of development, proliferation, metabolism, and transport. Among them, positive regulation of developmental process (GO: 0051094), negative regulation of developmental process (GO: 0051093), positive regulation of metabolic process (GO: 0009893), positive regulation of cell population proliferation (GO: 0008284), negative regulation of cell population proliferation (GO: 0008285), regulation of transport (GO: 0051049), and ion transport (GO: 0006811) were significantly enriched. GSEA showed that the significant negative enrichment of placenta development and the significant positive enrichment of multicellular organism metabolic process after PFHxS exposure compare to the control (Figure 4D; Figure S2A,B; Excel Table S12 and S19). A significant negative enrichment trend was present in amino acid transmembrane transport, amino acid transport, and anion transmembrane transport, despite the FDR >0.25 (Figure 4F,G; Figure S2C; Excel Table S12 and S19). Moreover, the SLC family, an important class of nutrient transporters, including some key amino acid transporters, *Slc1a5*, *Slc7a2*,
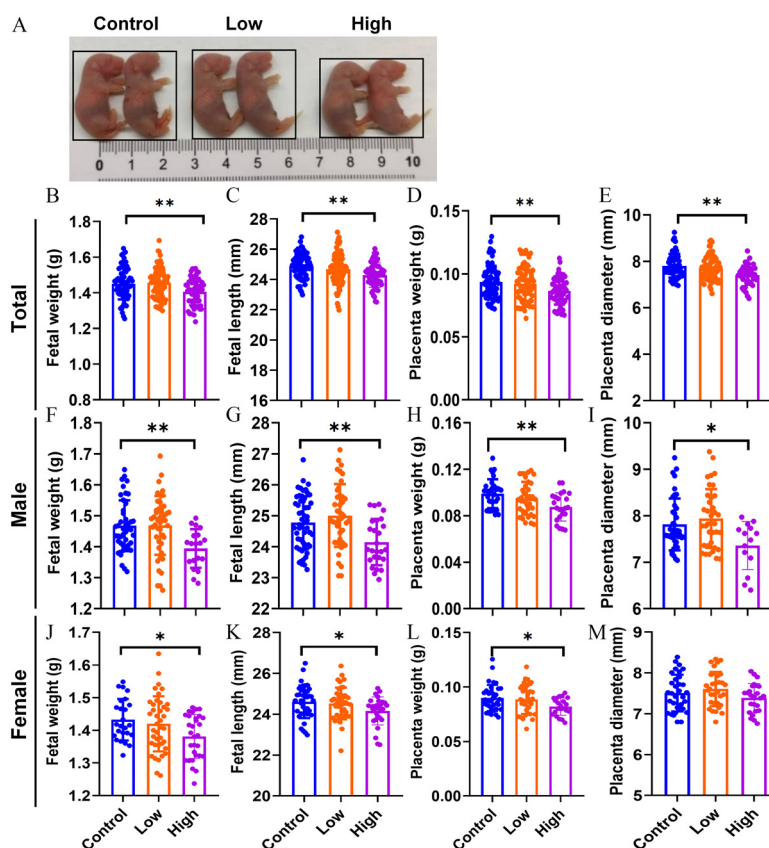
Figure 2. The effect of maternal PFHxS exposure on fetus and placenta (mean ± SEM; $n = 6$). The exposure doses were 0.3 (high) and 0.03 (low) μg/kg/day, which were administered in corn oil with 0.03% DMSO, and the control was corn oil with 0.03% DMSO. (A) Representative fetuses. (B) Total fetal weight. (C) Total fetal length. (D) Total placenta weight. (E) Total placenta diameter. (F) Male fetal weight. (G) Male total fetal length. (H) Male placenta weight. (I) Male placenta diameter. (J) Female fetal weight. (K) Female total fetal length. (L) Female placenta weight. (M) Female placenta diameter. *p*-Values were determined by one-way analysis of variance, [***]$p < 0.001$. Data in panels B–M are also presented in Excel Table S10. Note: GD, gestational day; DMSO, dimethyl sulfoxide; PFHxS, perfluorohexane sulfonate; SEM, standard error of mean.

Slc7a5, *Slc7a6*, *Slc7a7*, *Slc7a8*, *Slc7a11*, *Slc16a1*, *Slc36a4*, *Slc38a1*, *Slc38a6*, and *Slc38a10*, were enriched in core gene set of GSEA (Figure 4F,G; Figure S2C; Excel Table S12 and S19).

Signaling Pathways in the Placenta Whole-Genome

To identify and evaluate signal pathway changes during placenta development after PFHxS exposure, gene set variation analysis was performed in the whole genome of placenta. As shown in Figure 5A (Excel Table S13), pathways associated with development and proliferation, such as the canonical Wnt signaling pathway, positive regulation of mitogen-activated protein kinase (MAPK) cascade, positive regulation of development process, regulation of cellular response to growth factor stimulation, cell growth, negative regulation of growth, regulation of developmental growth, negative regulation of development process, angiogenesis, regulation of cell population proliferation, and positive regulation of cell population proliferation, were significantly positively enriched. In metabolism-related pathways, small molecule metabolic process, fatty acid metabolic process, cellular amino acid metabolic process, lipid metabolic process, and carbohydrate metabolism were significantly positively enriched. In transportation-related pathways, import into cells, positive regulation of transmembrane transport, and K^+ transmembrane transport were significantly negatively enriched, but negative regulation of transport was significantly positively enriched.

Furthermore, KEGG and Reactome analysis of DEGs were performed to evaluate signal pathway changes during placenta development after PFHxS exposure. As displayed in Figure 5B (Excel Table S13), DEGs were enriched in pathways of development and

proliferation, metabolic process, and cell fate, such as p53 signaling pathway (ko04115), TGFβ signaling pathway (ko04350), Wnt signaling pathway (ko04310), Hippo signaling pathway (ko04390), ferroptosis (ko04216), apoptosis (ko04210), folate biosynthesis (ko00790), arginine and proline metabolism (ko00330), tryptophan metabolism (ko00380), and glutathione metabolism (ko00480). KEGG pathway interaction analysis showed that TGFβ signaling pathway, Wnt signaling pathway, and metabolic pathways had major contributions and influenced other pathways (Figure 5C; Excel Table S13). As shown in Figure 5D (Excel Table S13), Reactome analysis also showed that DEGs were enriched in pathways of development and proliferation, metabolic process, transport, and cell fate, including signaling by TGFβ family members (R-MMU-9006936) and Wnt5a-dependent internalization of FZD2 and FZD5.

Identification of Signaling Pathways in the Placenta Development Processes

The above results have shown that expression of genes related to the biological processes of development, proliferation, metabolism, and transport were different compared to control after PFHxS exposure, but differences in the underlying signaling pathways remain to be clarified. To this end, we established four gene sets according to the distribution of DEGs in these biological processes. As displayed in Figure S3A–D (Excel Table S20), the heatmap showed the DEGs profile of development, metabolism, proliferation, and transport gene sets in placenta between the high-dose group and control. Further, KEGG and Reactome
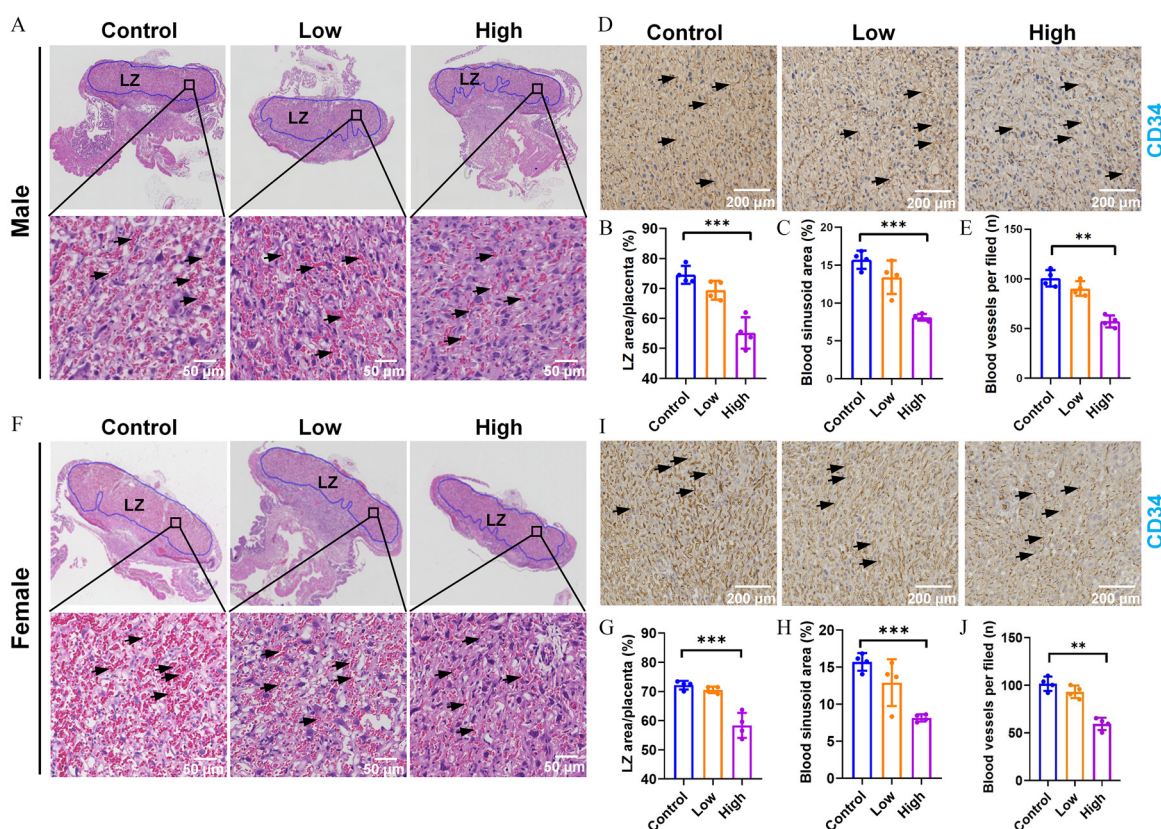
Figure 3. The effect of maternal PFHxS exposure on placental development (mean ± SEM; $n = 4$) at GD18. (A) Pathological morphology of male placenta. (B) Male LZ area placenta (%). (C) H&E staining picture for blood sinus and blood sinusoid area percentage (%) in male; magnification at $200\times$. (D) Immunohistology staining of blood vessel index marker CD34 in male. (E) Quantification for blood vessel marker CD34 per filed in male. (F) Pathological morphology of female placenta. (G) Female LZ area placenta (%). (H) H&E staining picture for blood sinus and blood sinusoid area percentage (%) in female; magnification at $200\times$. (I) Immunohistology staining of blood vessel index marker CD34 in female. (J) Quantification for blood vessel marker CD34 per filed in female. Black arrows in A and F indicate placental blood sinuses and in D and I indicate CD34-positive zones. p-Values were determined by one-way analysis of variance, $^{**}p < 0.01$, $^{***}p < 0.001$. Data in panels B, C, E, G, H, and J are also presented in Excel Table S11. Note: GD, gestational day; H&E, hematoxylin and eosin; LZ, labyrinth zone; PFHxS, perfluorohexane sulfonate; SEM, standard error of the mean.

analysis of four gene sets were performed to reveal the key signaling pathway. Among them, the signal pathways of development and proliferation were combined and displayed because of their high commonality. As shown in Figure 6A,B (Excel Table S14), DEGs from the development and proliferation gene set were evidently enriched in TGFβ signaling pathway (ko04350), Wnt signaling pathway (ko04310), signaling by TGFβ family members (R-MMU-9006936), and PI3K/AKT activation (R-MMU-198203). In the metabolic process gene set, DEGs were prominently enriched in the TGFβ signaling pathway (ko04350), cholesterol metabolism (ko04979), and AGE-RAGE signaling pathway in diabetic complications (ko04933) (Figure 6C,D; Excel Table S14). In the transport gene set, DEGs were markedly enriched in cholesterol metabolism (ko04979), protein digestion and absorption (ko04974), fat digestion and absorption (ko04975), transport of small molecules (R-MMU-382551), and SLC-mediated transmembrane transport (R-MMU-425407) (Figure 6E,F; Excel Table S14).

Furthermore, GSEA was performed based on the whole genome of placenta. As displayed in Figure 6G,H (Excel Table S14), the peroxisome proliferator-activated receptor (PPAR) signaling pathway was significantly positively enriched, and PPARγ had the greatest contribution in the core gene set. PPARα-targeted gene expression was significantly negatively enriched (Figure 6I; Excel Table S14). TGFβ (Figure S3E; Excel Table S20), p53 (Figure S3F; Excel Table S20), and Wnt (Figure S3G; Excel Table S20) signaling pathways were noticeable positively enriched. Further, UpSetR analysis was performed in four gene sets. As shown in

Figure S3H (Excel Table S20), the eight genes were shared by four gene sets. GO analysis showed that the biological functions of eight genes correspond to positive regulation of cell population proliferation (GO: 0008284), positive regulation of biological process (GO: 0048518), and positive regulation of metabolic process (GO: 0009893) (Figure S3I; Excel Table S20).

Genome-Wide Alternative Splicing Analyses following Gestational Exposure

To understand the mRNA integrity, AS analyses were performed from the placenta following gestational exposure. Here, we investigated the AS events in the biological process of placental development, including development, proliferation, metabolism, and transport. As displayed in Figure 7A (Excel Table S15), 1,141 differential AS events occurred in placenta with PFHxS exposure, including MXE, SE, RI, A3SS, and A5SS events. Separately, 1,344 and 1,491 differential AS events occurred in male and female placentae (Figure S4A,B; Excel Table S21). Among the five AS events, the number of differential SE events was the greatest, accounting for 59.9% and 59.22% of the total events in male and female placentae, respectively (Figure S4C; Excel Table S21). The role of these AS events in placental dysplasia was evaluated by GO analysis. As shown in Figure 7B (Excel Table S15), the genes with SE event were obviously enriched in the biological processes of development, proliferation, metabolism, and transport, including amino acid transport (GO: 0006865), transporter activity (GO:
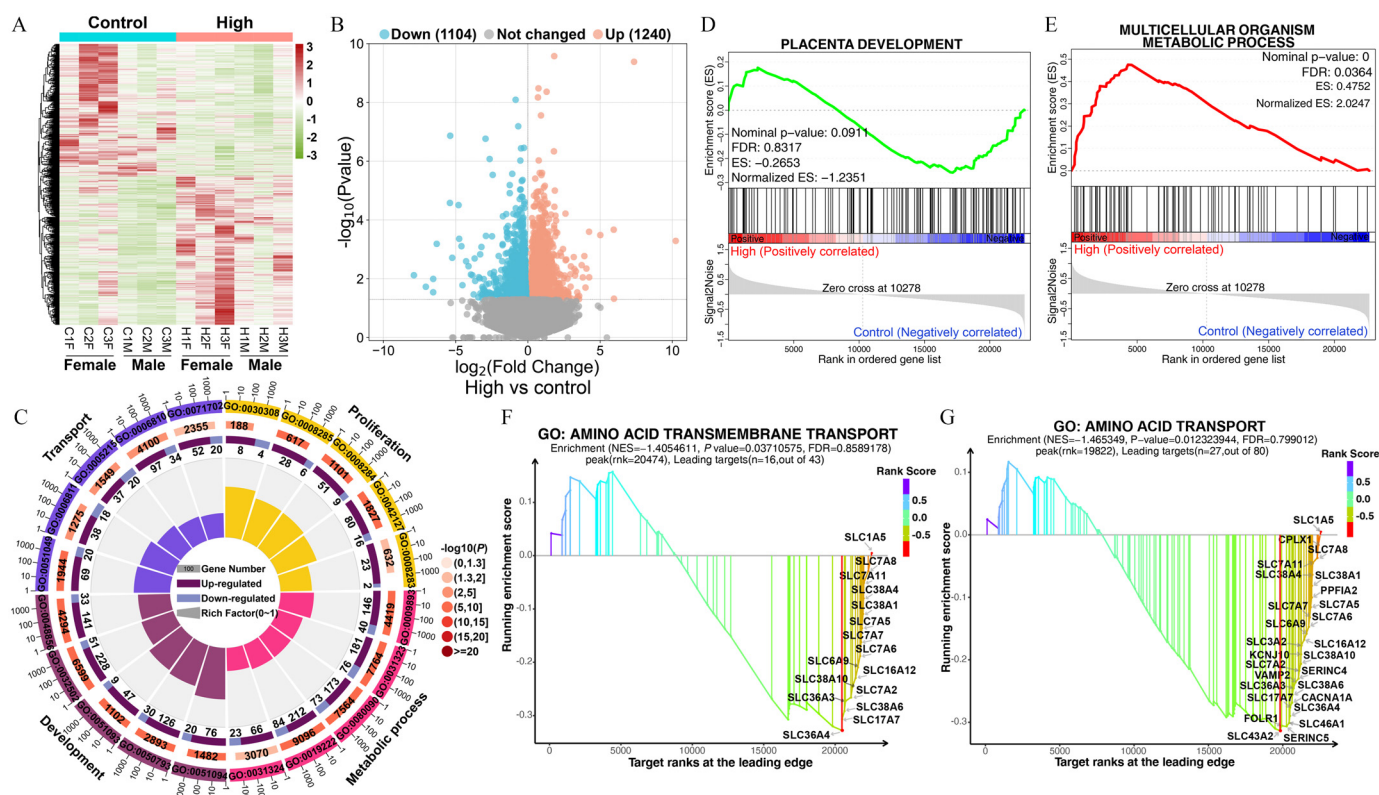
Figure 4. Placental RNA sequencing in high-dose group vs. control. (A) Heatmap showing the DEGs profile of placenta with high-dose group and control. (B) Volcano plot showing the DEGs distribution of placenta. (C) GO analysis. (D) GSEA showing the enrichment of placenta development in the high-dose group vs. control. (E) GSEA showing the enrichment of multicellular organism metabolic process in the high-dose group vs. control. (F) GSEA showing the enrichment of amino acid transmembrane transport in the high-dose group vs. control. (G) GSEA showing the enrichment of amino acid transport in the high-dose group vs. control. $n = 6$ in each group, including three males and three females. p-Values were determined by Wald test (B), hypergeometric test (C), or permutation test (D, E, F, G), and FDR values were determined by Benjamini-Hochberg method (D, E, F, G). Data in panels A–G are also presented in Excel Table S12. Note: DEGs, differentially expressed genes; FDR, false discovery rate; GO, Gene Ontology; GSEA, gene set enrichment analysis; PFHxS, perfluorohexane sulfonate.

0005215), and ion transport (GO: 0006811). In both male and female placentae, the genes with SE event were notably enriched in the biological processes of metabolism and transport compared to other AS events (Figure S4D,E; Excel Table S21). Similarly, the genes with MXE events or A3SS events were moderately enriched in the biological processes of development, proliferation, metabolism, and transport (Figure 7C,D; Excel Table S15). By contrast, the genes with RI events or A5SS were weakly enriched in the biological processes of development, metabolism, and transport and were not enriched in the process of proliferation (Figure 7E,F; Excel Table S15). Moreover, both in males and females, the expression profile of 42 key splicing factors were significantly different in placenta with PFHxS exposure compared to control (Figure S4F; Excel Table S21).

Further, KEGG and Reactome analyses were performed to assess the effect of AS on the signaling pathway of placental development. As shown in Figure S5A (Excel Table S22), in the RI gene set, the TGFβ signaling pathway, WNT signaling pathway, Hippo signaling pathway, Apelin signaling pathway, signaling pathways regulating pluripotency of stem cells, and ubiquitin-mediated proteolysis were enrichen and had major contributions. In the A3SS gene set, the MAPK signaling pathway, apoptosis, and TGFβ signaling pathway were enrichen and had major contributions (Figure S5B; Excel Table S22). In the A5SS gene set, the MAPK signaling pathway, WNT signaling pathway, and ubiquitin-mediated proteolysis were enrichen and had major contributions (Figure S5C; Excel Table S22). In the SE gene set, the MAPK signaling pathway, TGFβ signaling pathway, WNT signaling pathway, and

ubiquitin-mediated proteolysis were enriched and had major contributions (Figure S5D; Excel Table S22). In the MXE gene set, the MAPK signaling pathway and PI3K-AKT signaling pathway were enriched and had major contributions (Figure S5E; Excel Table S22). Similarly, Reactome analysis showed that the genes with AS events were enriched in development and proliferation, metabolism, and transport related pathways, including signaling by TGFβ family members, MAPK family signaling cascades, signaling by WNT, transport of small molecules, SLC-mediated transmembrane transport, metabolism of lipids, and fatty acid metabolism (Figure S5F; Excel Table S22). By contrast, the genes with SE event were strongly enriched in these pathways.

Effect of Gestational PFHxS Exposure on Placental Amino Acids Transport

Based on the transcriptome analysis, we hypothesized that that the obstruction of placental nutrient transport may be a key factor causing intrauterine growth restriction (IUGR) in response to PFHxS exposure. To test this hypothesis, the expression of 12 bidirectional amino acid and/or amide transporters[44,45] in placenta was measured by qRT-PCR. As shown in Figure 8A and Figure S6A (Excel Table S16 and S23), among the 12 bidirectional amino acid transporters, the expression levels of *Slc36a4*, *Slc38a10*, *Slc1a5*, *Slc7a2*, *Slc7a5*, *Slc7a6*, and *Slc7a7* were significantly lower in the placenta after PFHxS exposure. The expression of *Slc38a6* and *Slc7a11* also showed a downward trend in placenta after PFHxS exposure ($p = 0.051$ and $p = 0.053$). Subsequently, we annotated
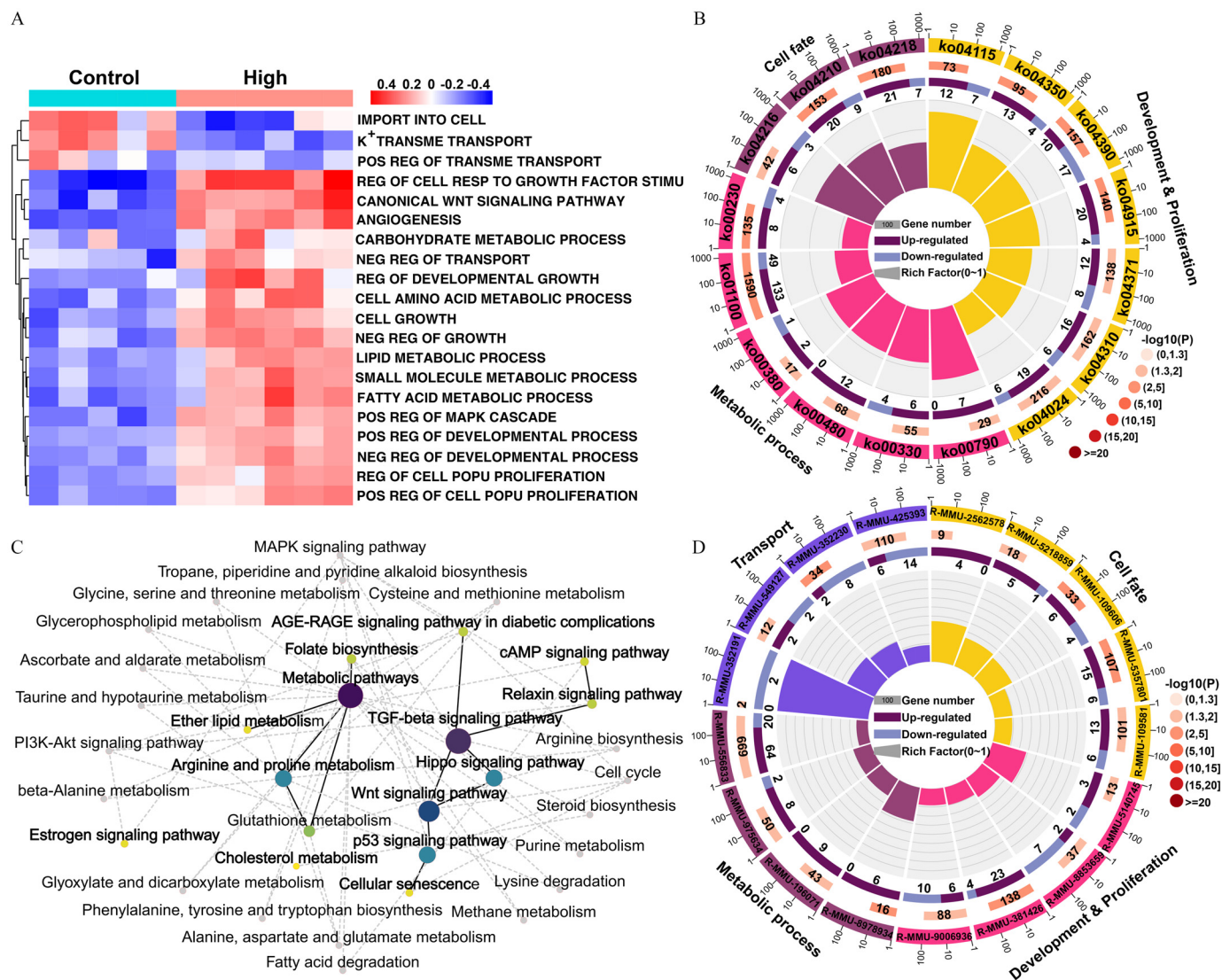
Figure 5. The enrichment analyses of key biological processes in the high-dose group vs. control. (A) GSVA based on GO database showing the differences in the biological processes in the high-dose group vs. control. (B) KEGG enrichment analysis of all DEGs. (C) KEGG pathway interaction analysis showing the relationship between DEG-enriched pathways. (D) Reactome enrichment analysis of all DEGs. $n = 6$ in each group, including three males and three females. p-Values were determined by hypergeometric test (B and D). Data in panels A–D are also presented in Excel Table S13. Note: DEGs, differentially expressed genes; GO, gene ontology; GSVA, gene set variation analysis; KEGG, Kyoto Encyclopedia of Genes and Genomes; PFHxS, perfluorohexane sulfonate.

the specific functions of these seven amino acid transporters. As shown in Figure 8B (Excel Table S16), these amino acid transporters mediate the transport of 29 amino acids, including six basic amino acids, seven acidic amino acids, and 16 neutral amino acids, as well as two amides. Further, the contents of 29 amino acids and 44 amides in the placenta were quantified by LC-MS/MS. As displayed in Figure 8C (Excel Table S16), the contents of eight essential amino acids, 21 nonessential amino acids, and 44 amides in placenta after PFHxS exposure were significantly lower than those in control. Similarly, the contents of those amino acids and amides in male and female placentae after PFHxS exposure were lower than in the control (Figure S6B,C; Excel Table S23).

Further, we investigated the effect of AS on amino acid transport in the placenta. As displayed in Figure 9A,D,G (Excel Table S17), SE events of the skipped third exon of *Slc1a5* and the skipped fourth exon of *Slc7a7* and RI events of the fourth intron retention in placenta after PFHxS exposure were markedly higher than in the control. Subsequently, 3D structures of Slc1a5, Slc7a6, and Slc7a7 splicing variants were simulated using AlphaFold2 based on a machine learning approach.[46] As shown in Figure 9B,E,H, 3D

structures of Slc1a5, Slc7a6, and Slc7a7 prototype and splicing variant were visualized, respectively. Then, structural differences between these protein prototypes and splicing variants were evaluated. As shown in Figure 9C, the splicing variant of Slc1a5 lacked a β-pleated sheet in the 207–221 nontransmembrane region of the amino acid chain (the red part) compared to the prototype. The splicing variant of Slc7a6 lacked six α-helices in the 296–515 transmembrane region of the amino acid chain compared to the prototype (Figure 9F). The splicing variant of Slc7a7 lacked four α-helices in the 352–510 transmembrane region of the amino acid chain compared to the prototype (Figure 9I). These results suggested significant changes in the structure and activity of Slc1a5, Slc7a6, and Slc7a7 proteins in placenta after PFHxS exposure due to the occurrence of AS events.

Discussion

To our knowledge, this is the first animal study evaluating the developmental toxicology of PFHxS, an environmentally ubiquitous PFAS congener frequently detected among pregnant women, upon
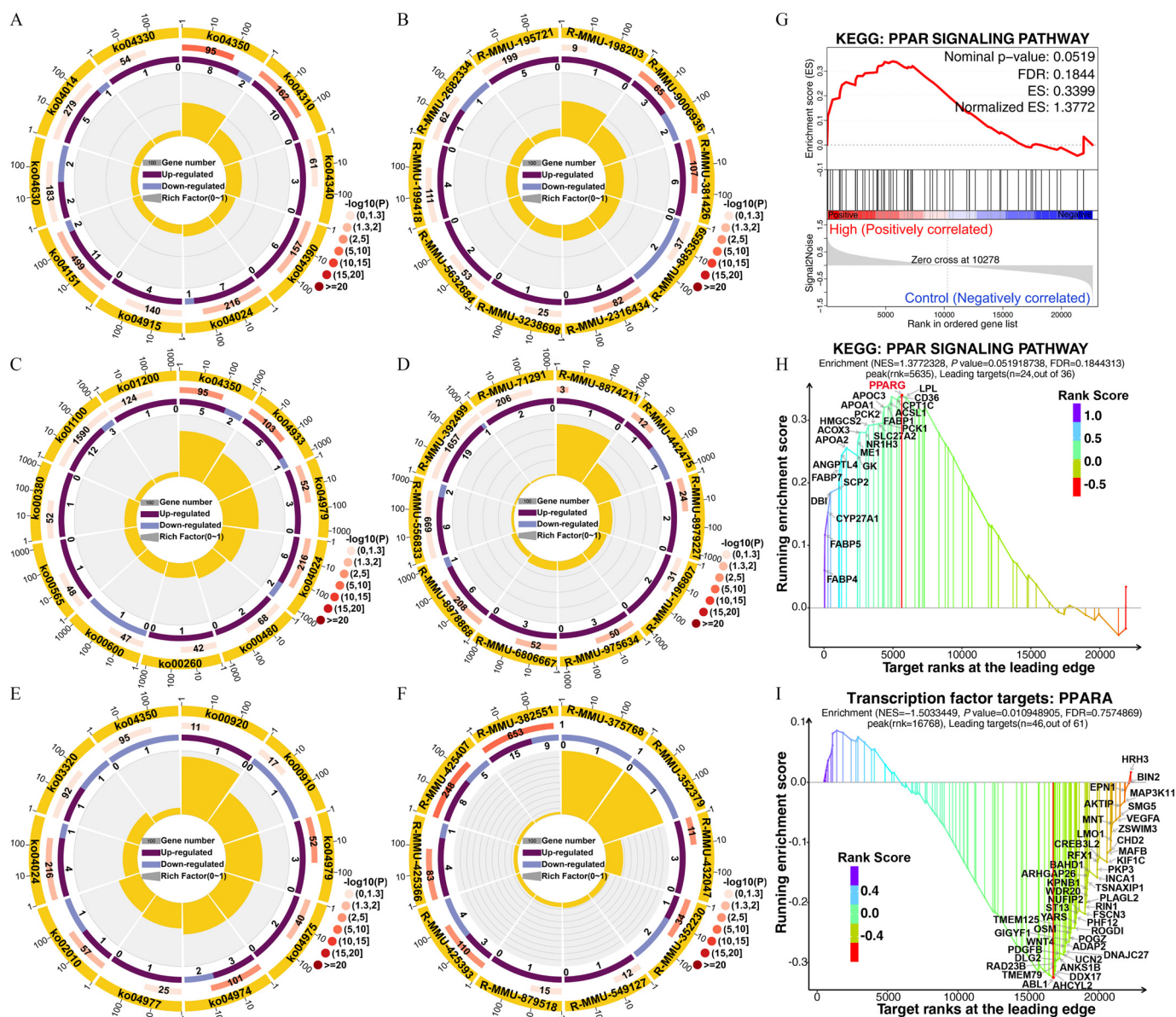
Figure 6. Key pathway enrichment analyses in placenta development-related processes. (A) KEGG enrichment analysis of DEGs in development and proliferation processes. (B) Reactome enrichment analysis of DEGs in development and proliferation processes. (C) KEGG enrichment analysis of DEGs in metabolic process. (D) Reactome enrichment analysis of DEGs in the metabolic process. (E) KEGG enrichment analysis of DEGs in transport process. (F) Reactome enrichment analysis of DEGs in transport process. (G) GSEA showing the enrichment of PPAR signaling pathway in the high-dose group vs. control. (H) The distribution of core genes in GSEA for PPAR signaling pathway. (I) GSEA showing the enrichment of PPARα-targeted gene transcription in the high-dose group vs. control. $n = 6$ in each group, including three males and three females. p-Values were determined by hypergeometric test (A–F) or permutation test (G and H), and FDR values were determined by Benjamini-Hochberg method (G and H). Data in panels A–I are also presented in Excel Table S14. Notes: GSEA, gene set enrichment analysis; KEGG, Kyoto Encyclopedia of Genes and Genomes; PFHxS, perfluorohexane sulfonate; PPAR, peroxisome proliferator-activated receptor.

gestational exposure at human-relevant low doses in terrestrial mammals. Mice exposed to PFHxS *in utero* exhibited signs of IUGR as well as impaired placental development. Our multiomics approach combining gene expression and alternative splicing offers a lens to study mRNA quantity and quality, suggesting that dams exposed to PFHxS had disruptions in the key biological processes of placental development, proliferation, metabolism, and transport, potentially explaining the key toxicity phenotype of IUGR during *in utero* development. Further detection of the expression and differential AS events of placental key transporter genes, protein structure simulation of AS variants, as well as amino acid and amide metabolite levels demonstrated that PFHxS exposure during pregnancy led to impairment of placental amino acid

transport. In summary, we conclude that exposure to human-relevant PFHxS exposure during pregnancy was associated with IUGR likely via impairment of placental amino acid transport by AS-induced changes of transporter structure and activity and down-regulation of their expression, and thereby impairment of placental development. This approach can be important in future toxicological studies, as it offers insights into both the expression level and mRNA integrity, which subsequently dictates protein structure and bioactivity upon environmental insults.

Increasing human studies show that PFHxS is detected in the placenta and umbilical cord blood,[24,47] which are consistent with our animal results. However, whether the transmembrane is affected by exposure at a human-relevant low dose has not been fully
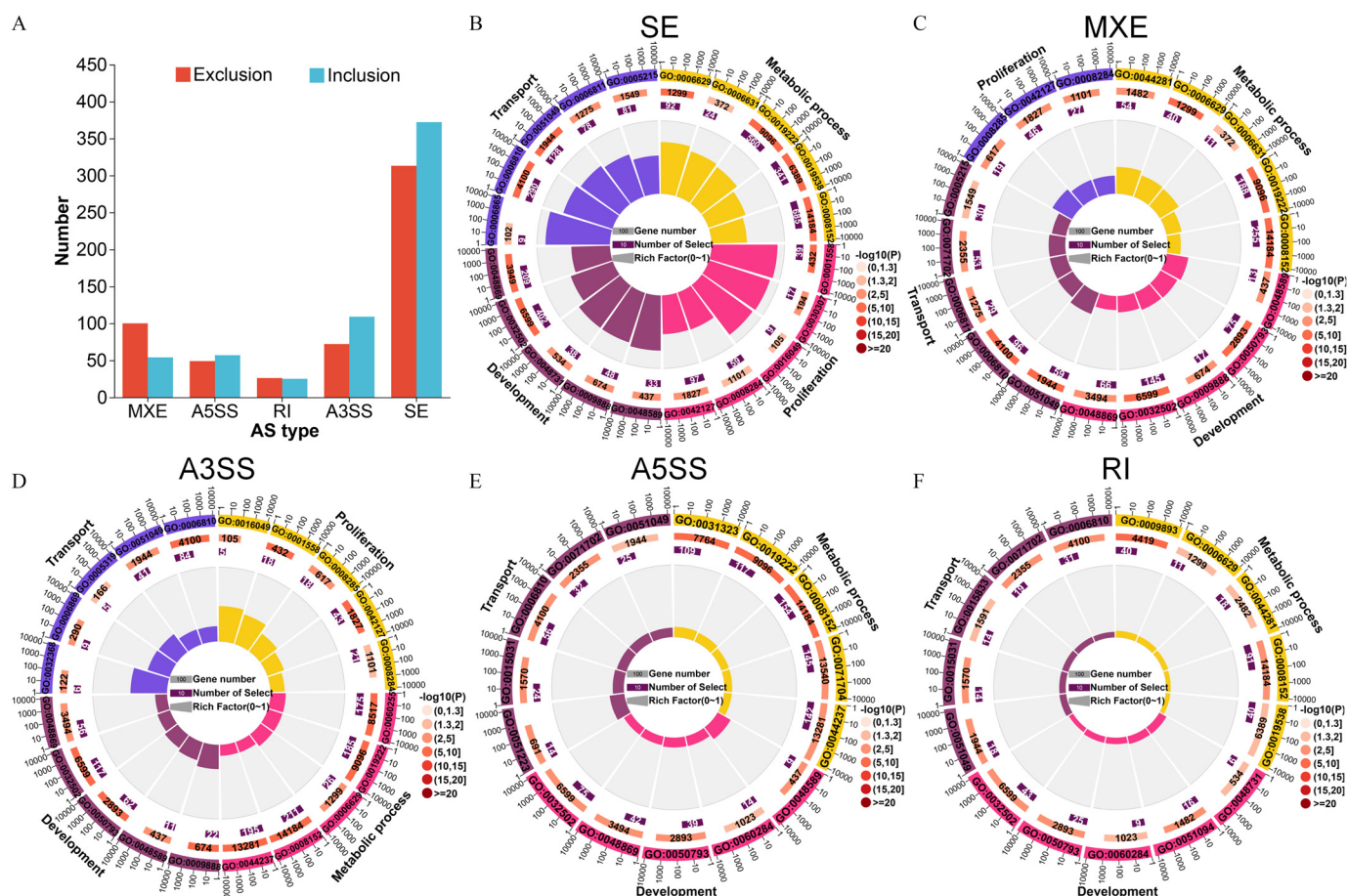
Figure 7. AS analyses of placental development process in the high-dose group vs. control. (A) The number of differential AS events in placenta with PFHxS exposure compared to control. (B) GO enrichment analysis of the genes with SE event. (C) GO enrichment analysis of the genes with MXE event. (D) GO enrichment analysis of the genes with A3SS event. (E) GO enrichment analysis of the genes with A5SS event. (F) GO enrichment analysis of the genes with RI event. $n = 6$ in each group, including three males and three females. p-Values were determined by hypergeometric test (B–F). Data in panels A–F are also presented in Excel Table S15. Note: A3SS, alternative 3' splice site; A5SS, alternative 5' splice site; AS, alternative splicing; GO, Gene Onotology; GSEA, gene set enrichment analysis; MXE, mutually exclusion exon; PFHxS, perfluorohexane sulfonate; RI, retained intron; SE, skipped exon.

resolved. Here, we observed higher levels of PFHxS in the placenta and fetus of exposed dams than in the control in this model and that this appeared to be dose dependent. These results further confirmed that PFHxS could pass across the placental barrier and reach the fetus. Previous reports have demonstrated that PFAS chemicals including PFHxS may penetrate the placental barrier via transporters including organic anion transporter 4 (OAT4), p-glycoprotein (MDR1), and multi-drug resistance-associated protein 2 (MRP2).[48,49] However, further work is needed to identify key transporters and to elucidate their roles in the body distribution of PFHxS across the placenta. Nevertheless, our results provide some new insights into the penetration of PFHxS in placenta in animal models.

To the best of our knowledge, this is the first study reporting the developmental toxicity of PFHxS at human-relevant doses resulting in growth restriction in a terrestrial model. PFHxS is structurally stable with low hydrophilicity, so it has high bioaccumulation and persistence in biological systems.[3] It has become one of the most frequently reported PFAS chemicals in widespread human and environmental samples.[1,50] Human studies have suggested that PFHxS exposure is associated with many adverse health outcomes. Studies demonstrated that PFAS exposure during pregnancy is related to negative health outcomes in pregnancy, childbirth, and later life and increases the incidence of gestational diabetes mellitus, childhood obesity, preeclampsia, and fetal

growth restriction,[51] as well as testicular function of offspring mice.[30] However, the causal relationship between exposure to the chemical and developmental toxicity remain unknown. Our mouse model suggests that PFHxS exposure in mice during pregnancy impaired pregnancy outcomes and increased the risk of IUGR, which is characterized by decreased fetal weight and body length in fetal mice. This work fills the gap in the study of developmental toxicity of PFHxS exposure during pregnancy.

Placenta plays an important role in maintaining maternal health and embryonic development, involving nutrition supply and exchange to ensure the normal development of the fetus.[51] Studies suggest that maternal exposure to a major congener PFOA can induce incidence of placental and fetus abnormalities as well as lead to atrophy or necrosis of placental maze layer and early fibrin clot formation.[52] In our study, we found that PFHxS-exposed dams had lower placental weight and smaller diameter compared to controls, which is consistent with the above findings. Furthermore, we found that compared with the control group, the placental maze layer area, sinus area, and protein expression of vascular biomarker CD34 were significantly lower in exposed mice. Fetal nutrition depends on the labyrinthine layer, acquiring nutrients via the branch of placental trophoblast cells located between maternal blood and fetal blood vessels.[53] The results of our study suggest that PFHxS interfered with the formation of placental labyrinthine layer and blood vessels, thus further causing placental dysfunction.
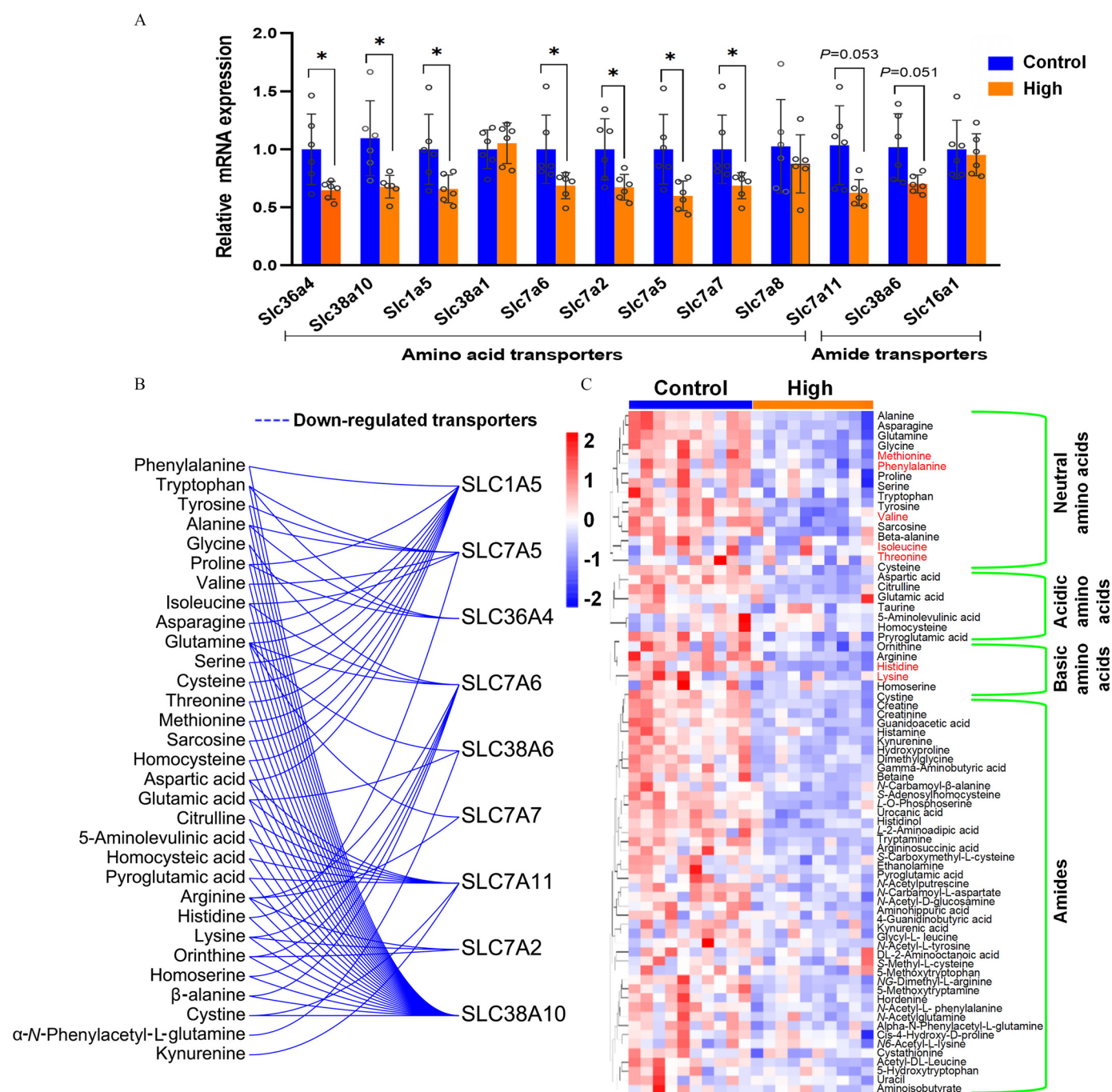
Figure 8. Evaluation of placental amino acid transport in the high-dose group and control. (A) The mRNA expression of 12 amino acid transporters in placenta ($n = 6$ in each group). (B) Functional annotation of seven amino acid transporters. (C) The profile of 29 amino acids and 44 amides in placenta ($n = 10$ in each group, five males and five females). *p*-Values were determined by Student's *t* test (A), *$p < 0.05$. Data in panels A–C are also presented in Excel Table S16. Note: PFHxS, perfluorohexane sulfonate.

In addition, the histopathological destruction of placenta may lead to hypoxia, poor fetal perfusion, and poor maternal perfusion, which may further lead to limited fetal intrauterine formation.[54] The demand for nutrition for fetal development may then exceed the supply from the placenta, which leads to limited fetal development. These results suggest that placenta is at least a part of the target organ of PFHxS, and placental dysplasia may be responsible for IUGR in the fetus following gestational exposure.

Transcriptome analysis provides a comprehensive picture of changes in the placenta in response to environmental exposures, including direct damage and some long-term hazards.[55,56] Based on this, the changes of placental genome-wide expression and their contribution to placental dysplasia and IUGR due to PFHxS exposure were comprehensively evaluated. Several vital biological processes, including development, proliferation, metabolism, and transport, were identified with significant differences between control and exposed animals. Some seemingly contradictory changes in these biological processes, such as positive and negative regulation of developmental process, as well as positive and negative regulation of cell population proliferation were up-enriched, indicating likely catch-up growth of the placenta in the state of dysplasia.[57,58] Furthermore, upregulations of metabolic processes
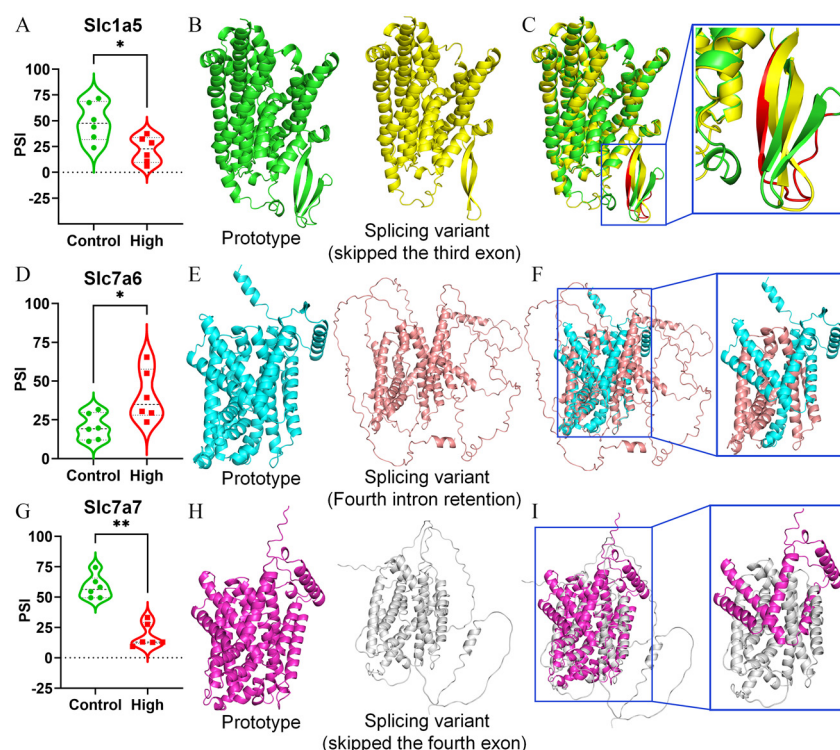
Figure 9. The effect of alternative splicing on simulated structures of amino acid transporters using AlphaFold2 following PFHxS exposure. (A) Violin plot showing the PSI values of the skipped-third exon in *Slc1a5* transcripts. (B) The 3D structure of Slc1a5 prototype and splicing variant. (C) Structural differences between Slc1a5 prototype and splicing variant. (D) Violin plot showing the PSI values of the fourth intron retention in *Slc7a6* transcripts. (E) The 3D structure of Slc7a6 prototype and splicing variant. (F) Structural differences between Slc7a6 prototype and splicing variant. (G) Violin plot showing the PSI values of the skipped-fourth exon in *Slc7a7* transcripts. (H) The 3D structure of Slc7a7 prototype and splicing variant. (I) Structural differences between Slc7a7 prototype and splicing variant. $n = 6$ in each group; the *p*-values were determined Mann-Whitney *U*-test (A, D, and G), $^*p < 0.05$, $^{**}p < 0.01$. Data in panels A, D, and G are also presented in Excel Table S17. Note: 3D, three-dimensional; PFHxS, perfluorohexane sulfonate; PSI, percent spliced-in.

also contribute to the catch-up growth of the placenta. Notably, obstructed nutrient transport might be the key cause of placental dysplasia due to downregulation in many SLC family transporter proteins,[59,60] and this was further emphasized as amino acid transmembrane transport and placental development showed a similar negative trend.

The physiopathological effects of genome-wide expression alterations depend on the switching of signaling pathways on and off.[61] We performed the DEG enrichment analysis in the KEGG and Reactome pathway databases, as well as a gene set analysis called GSVA. Based on this, some critical pathway alterations in response to PFHxS exposure were identified. Several positive transport-related pathways, including import into cell, positive regulation of transmembrane transport, and K^+ transmembrane transport were downregulated in response to PFHxS exposure, yet negative regulation of transport was upregulated. These results suggest that transport process was obstructed in placenta caused by PFHxS exposure, consistent with the findings described above. In addition, the upregulation of metabolism, development and proliferation, and cell fate-related pathways further indicated the catch-up growth of the placenta in the state of dysplasia. Notably, the impairment on nutrient transport in the placenta by PFHxS were mostly enriched toward amino acids and ions, and their impacts on other major nutrients including lipids, sugars, and other nutrients were relatively minimal in our results.
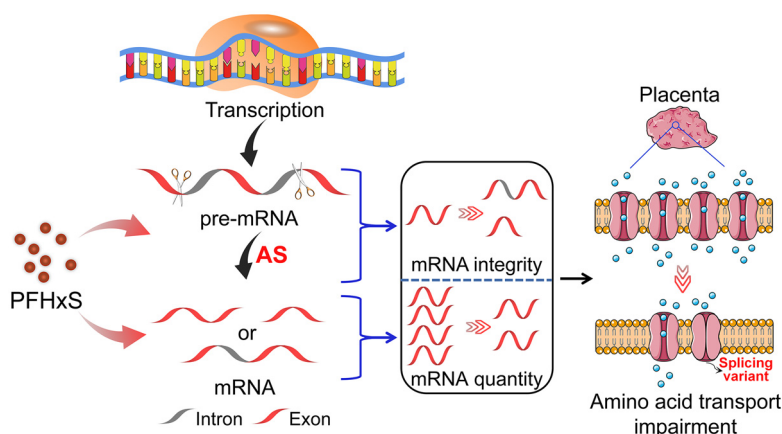

Figure 10. Proposed mechanism of actions. Note: AS, alternative splicing.

The mRNA quantity represents gene transcriptional activity and also maps the activity of signaling pathways and biological processes.[62,63] Enrichment analysis of gene sets established based on DEG distribution is beneficial to reveal the change of signaling pathways in a biological process.[64] Enrichment analysis of development and proliferation gene sets showed significant up-regulation of the TGFβ signaling pathway, and a similar result appeared in the metabolic process gene set. These findings suggested that the TGFβ signaling pathway might be a critical transponder in response to PFHxS exposure, possibly mediating the catch-up growth of the placenta in the dysplastic state by upregulation of developmental, proliferative, and metabolic processes. Also noteworthy, the PPAR signaling pathway was significantly positively enriched, and PPARγ had the greatest contribution in the PPAR pathway core gene set, and PPARα-targeted gene expression was significantly negatively enriched. These data suggest that PPARγ was the primary factor in response to PFHxS rather than PPARα in the placenta. In the transport gene set, DEGs were enriched not only in transport-related pathways but also in some metabolism-related pathways, indicating that changes in transport processes might be associated with alterations in metabolic processes. Moreover, the eight shared genes were involved in the positive regulation of metabolism, cell proliferation, and biological process, suggesting the interaction of these biological processes.

The mRNA integrity determines the posttranscriptional activity of genes.[65] AS is a splicing mechanism that determines mRNA integrity, which alters the mRNA sequences, resulting in changes in the structure, activity, binding specificity, or distribution of proteins.[66–68] Our results suggested disrupted AS coding signal transfer, i.e., unfavorable crosstalk, in the placental biological processes of development, proliferation, metabolism, and transport due to PFHxS exposure, which was consistent with the results of transcriptomic analysis. Compared with other AS events, SE events showed a stronger effect on these biological processes. Moreover, the genes with SE events were significantly enriched in transport process, including amino acid transport, transporter activity, and ion transport, indicating that SE events might be the key mechanism mediating the obstruction of placental nutrient transport caused by PFHxS exposure. In addition, these AS events were clustered in development-, proliferation-, and metabolism-related pathways, suggesting that they might contribute to placental catch-up growth. Among them, these AS events mainly affected the TGFβ signaling pathway, MAPK signaling pathway, and Wnt signaling pathway, because these pathways presented a distinct cluster of AS events. The 3D structure simulation of key transporter genes with the occurrence of AS using AlphaFold2 supported our hypothesis of impaired nutrient transportation in the placenta induced by PFHxS exposure during pregnancy.

Amino acids are the material basis for functional protein synthesis and are essential nutrients in fetal development. During pregnancy, the placenta acts as a bridge to transfer nutrients from the mother to the fetus, maintaining fetal development. The impaired placental transport function can be a direct cause of fetal malnutrition and eventually IUGR.[69,70] Notably, maternal exposure to environmental pollutants such as arsenic, cadmium, and 1-nitropyrene during pregnancy impairs placental development and function.[71–73] Results from this study suggest that placental transport function was impaired after PFHxS exposure and led to IUGR. Based on DEG and AS analyses, we identified quantitative and qualitative differences in the mRNA of some placental amino acid transporters in PFHxS-exposed vs. control animals. Amino acid transporters were expressed at a significantly lower level in the placenta after PFHxS exposure. Subsequently,

data on essential and nonessential amino acids confirmed that nutrient transportation across the placenta was impaired in exposed animals, explaining the findings from DEG and AS findings. In summary, we revealed that PFHxS-exposed animals exhibited impaired placental amino acid transport, possibly by AS-induced differences in transporter structure and activity and down-regulating transporter gene expression, which may be a mechanism contributing to IUGR in the fetus (Figure 10).

The implications of the study should be emphasized. First, developmental toxicological studies have always focused on two major congeners PFOS and PFOA, yet the wide environmental occurrence and increasing exposure burden of PFHxS in humans are in huge contrast to the scarcity of animal toxicological studies to confirm the causal relationship. Second, the dose selected in our study was based on real human internal exposure burden, which is highly relevant to humans including during pregnancy. More significantly, comparing our selected dose for effect of IUGR (0.3 μg/kg/day) with available data for PFOS (2.5 mg/kg/day)[27] or PFOA (5 mg/kg/day) in mice,[28] the substitute chemical PFHxS for PFOS demonstrated magnitudes higher developmental toxicity and may question the suitability of PFHxS as a safe substitute. Third, the quantity and integrity of mRNA represent the transcriptional activity and posttranscriptional activity of genes and dictates their biological activity.[65,74] Transcriptome analysis based on changes in mRNA quantity, including DEGs and gene set enrichment analysis, is a series of "quantity-effect" evaluations.[75] In contrast, AS analysis aims to elucidate mRNA integrity changes and their effects on biological processes and signaling pathways and is a series of "quality-effect" evaluations.[76] Therefore, genome-wide expression and AS analyses facilitates comprehensive understanding of the biological process and signaling pathway alterations in response to PFHxS exposure. Nevertheless, future gene editing techniques implemented both *in vivo* and *in vitro* to specifically express these AS isomers are encouraged to investigate how these induced isomers may impact cell growth and placenta development. Placental and fetal levels of amino acids and amides in the gene-edited AS isomers may provide stronger evidence in future work. One of the limitations to be acknowledged is that here we focused primarily on the impairment of the placenta and less on the fetus. Although placenta is an important nutrient supply for fetal development, the precise mechanism underlying developmental toxicity of PFHxS toward the fetus, particularly based on human studies, is insufficiently understood and may require future in-depth research. Future work is also needed to further explore the toxicological mechanisms underpinning placental development, particularly at different gestational stages, and the reprogramming of metabolic processes impacting long-term offspring health using various technological approaches.[77]

Conclusion

Taken together, this study reports, to our knowledge for the first time, that mice gestationally exposed to human-relevant doses of environmentally ubiquitous PFHxS exhibited developmental toxicity at exposure doses magnitudes lower than reported for PFOS[27] or PFOA[28] via impairment of placental development in mice. Our multiomics research approach of combining gene expression and alternative splicing provides a lens of understanding mRNAs from both their quantity and quality/integrity leading to protein bioactivity as verified by protein structure simulation. Our work confirms epidemiological findings and question the suitability of using PFHxS as an industrial substitute to PFOS. This work calls for future attention on the health risk of this persistent yet ubiquitous chemical in the early developmental stage and provides a new approach for understanding gene expression

from both a quantitative and qualitative omics approach in toxicological studies.

References

1. Domingo JL, Nadal M. 2019. Human exposure to per- and polyfluoroalkyl substances (PFAS) through drinking water: a review of the recent scientific literature. Environ Res 177:108648, PMID: 31421451, https://doi.org/10.1016/j.envres.2019.108648.
2. Barhoumi B, Sander SG, Tolosa I. 2022. A review on per- and polyfluorinated alkyl substances (PFASs) in microplastic and food-contact materials. Environ Res 206:112595, PMID: 34929191, https://doi.org/10.1016/j.envres.2021.112595.
3. Evich MG, Davis MJB, McCord JP, Acrey B, Awkerman JA, Knappe DRU, et al. 2022. Per- and polyfluoroalkyl substances in the environment. Science 375(6580):eabg9065, PMID: 35113710, https://doi.org/10.1126/science.abg9065.
4. EU (European Union). 2019. *Regulation (EU) 2019/1021 of the European Parliament and of the Council of 20 June 2019 on Persistent Organic Pollutants (Recast) (Text with EEA Relevance)*. https://eur-lex.europa.eu/legal-content/EN/TXT/?uri=CELEX%3A32019R1021&qid=1698308501250 [accessed 26 October 2023].
5. Xie LN, Wang XC, Dong XJ, Su LQ, Zhu HJ, Wang C, et al. 2021. Concentration, spatial distribution, and health risk assessment of PFASs in serum of teenagers, tap water and soil near a Chinese fluorochemical industrial plant. Environ Int 146:106166, PMID: 33068851, https://doi.org/10.1016/j.envint.2020.106166.
6. Gockener B, Weber T, Rudel H, Bucking M, Kolossa-Gehring M. 2020. Human biomonitoring of per- and polyfluoroalkyl substances in German blood plasma samples from 1982 to 2019. Environ Int 145:106123, PMID: 32949877, https://doi.org/10.1016/j.envint.2020.106123.
7. Zhang Y, Beesoon S, Zhu L, Martin JW. 2013. Biomonitoring of perfluoroalkyl acids in human urine and estimates of biological half-life. Environ Sci Technol 47(18):10619–10627, PMID: 23980546, https://doi.org/10.1021/es401905e.
8. Fujii Y, Harada KH, Koizumi A. 2013. Occurrence of perfluorinated carboxylic acids (PFCAs) in personal care products and compounding agents. Chemosphere 93(3):538–544, PMID: 23932147, https://doi.org/10.1016/j.chemosphere.2013.06.049.
9. van Beijsterveldt I, van Zelst BD, van den Berg SAA, de Fluiter KS, van der Steen M, Hokken-Koelega ACS. 2022. Longitudinal poly- and perfluoroalkyl substances (PFAS) levels in Dutch infants. Environ Int 160:107068, PMID: 34968992, https://doi.org/10.1016/j.envint.2021.107068.
10. Mamsen LS, Bjorvang RD, Mucs D, Vinnars MT, Papadogiannakis N, Lindh CH, et al. 2019. Concentrations of perfluoroalkyl substances (PFASs) in human embryonic and fetal organs from first, second, and third trimester pregnancies. Environ Int 124:482–492, PMID: 30684806, https://doi.org/10.1016/j.envint.2019.01.010.
11. Varsi K, Huber S, Averina M, Brox J, Bjorke-Monsen AL. 2022. Quantitation of linear and branched perfluoroalkane sulfonic acids (PFSAs) in women and infants during pregnancy and lactation. Environ Int 160:107065, PMID: 34959199, https://doi.org/10.1016/j.envint.2021.107065.
12. Sunderland EM, Hu XC, Dassuncao C, Tokranov AK, Wagner CC, Allen JG. 2019. A review of the pathways of human exposure to poly- and perfluoroalkyl substances (PFASs) and present understanding of health effects. J Expo Sci Environ Epidemiol 29(2):131–147, PMID: 30470793, https://doi.org/10.1038/s41370-018-0094-1.
13. Makey CM, Webster TF, Martin JW, Shoeib M, Harner T, Dix-Cooper L, et al. 2017. Airborne precursors predict maternal serum perfluoroalkyl acid concentrations. Environ Sci Technol 51(13):7667–7675, PMID: 28535063, https://doi.org/10.1021/acs.est.7b00615.
14. Marques ES, Agudelo J, Kaye EM, Modaresi SMS, Pfohl M, Becanova J, et al. 2021. The role of maternal high fat diet on mouse pup metabolic endpoints following perinatal PFAS and PFAS mixture exposure. Toxicology 462:152921, PMID: 34464680, https://doi.org/10.1016/j.tox.2021.152921.
15. Preston EV, Webster TF, Claus Henn B, McClean MD, Gennings C, Oken E, et al. 2020. Prenatal exposure to per- and polyfluoroalkyl substances and maternal and neonatal thyroid function in the project viva cohort: a mixtures approach. Environ Int 139:105728, PMID: 32311629, https://doi.org/10.1016/j.envint.2020.105728.
16. Hall SM, Zhang S, Hoffman K, Miranda ML, Stapleton HM. 2022. Concentrations of per- and polyfluoroalkyl substances (PFAS) in human placental tissues and associations with birth outcomes. Chemosphere 295:133873, PMID: 35143854, https://doi.org/10.1016/j.chemosphere.2022.133873.
17. Kobayashi S, Azumi K, Goudarzi H, Araki A, Miyashita C, Kobayashi S, et al. 2017. Effects of prenatal perfluoroalkyl acid exposure on cord blood IGF2/H19 methylation and ponderal index: the Hokkaido study. J Expo Sci Environ Epidemiol 27(3):251–259, PMID: 27553991, https://doi.org/10.1038/jes.2016.50.
18. Borghese MM, Walker M, Helewa ME, Fraser WD, Arbuckle TE. 2020. Association of perfluoroalkyl substances with gestational hypertension and preeclampsia in the MIREC study. Environ Int 141:105789, PMID: 32408216, https://doi.org/10.1016/j.envint.2020.105789.
19. Preston EV, Hivert MF, Fleisch AF, Calafat AM, Sagiv SK, Perng W, et al. 2022. Early-pregnancy plasma per- and polyfluoroalkyl substance (PFAS) concentrations and hypertensive disorders of pregnancy in the Project Viva cohort. Environ Int 165:107335, PMID: 35696844, https://doi.org/10.1016/j.envint.2022.107335.
20. Grellier J, Bennett J, Patelarou E, Smith RB, Toledano MB, Rushton L, et al. 2010. Exposure to disinfection by-products, fetal growth, and prematurity: a systematic review and meta-analysis. Epidemiology 21(3):300–313, PMID: 20375841, https://doi.org/10.1097/EDE.0b013e3181d61ffd.
21. Fan Y, Guo L, Wang R, Xu J, Fang Y, Wang W, et al. 2023. Low transplacental transfer of PFASs in the small-for-gestational-age (SGA) new-borns: evidence from a Chinese birth cohort. Chemosphere 340:139964, PMID: 37633609, https://doi.org/10.1016/j.chemosphere.2023.139964.
22. Ma L. 2009. Endocrine disruptors in female reproductive tract development and carcinogenesis. Trends Endocrinol Metab 20(7):357–363, PMID: 19709900, https://doi.org/10.1016/j.tem.2009.03.009.
23. EU (European Union). 2022. *Council Decision (EU) 2022/997 of 7 April 2022 on the Position to be Taken on Behalf of the European Union at the Tenth Meeting of the Conference of the Parties to the Stockholm Convention on Persistent Organic Pollutants as Regards the Proposal for Amendment of Annex A to that Convention*. https://eur-lex.europa.eu/legal-content/EN/TXT/?uri=CELEX:32022D0997 [accessed 3 August 2023].
24. Chen F, Yin S, Kelly BC, Liu W. 2017. Isomer-specific transplacental transfer of perfluoroalkyl acids: results from a survey of paired maternal, cord sera, and placentas. Environ Sci Technol 51(10):5756–5763, PMID: 28434222, https://doi.org/10.1021/acs.est.7b00268.
25. Yao W, Xu J, Tang W, Gao C, Tao L, Yu J, et al. 2023. Developmental toxicity of perfluorohexane sulfonate at human relevant dose during pregnancy via disruption in placental lipid homeostasis. Environ Int 177:108014, PMID: 37315490, https://doi.org/10.1016/j.envint.2023.108014.
26. Šabović I, Cosci I, De Toni L, Ferramosca A, Stornaiuolo M, Di Nisio A, et al. 2020. Perfluoro-octanoic acid impairs sperm motility through the alteration of plasma membrane. J Endocrinol Invest 43(5):641–652, PMID: 31776969, https://doi.org/10.1007/s40618-019-01152-0.
27. Li J, Quan XJ, Chen G, Hong JW, Wang Q, Xu LL, et al. 2020. PFOS-induced placental cell growth inhibition is partially mediated by lncRNA H19 through interacting with miR-19a and miR-19b. Chemosphere 261:127640, PMID: 32738709, https://doi.org/10.1016/j.chemosphere.2020.127640.
28. Huang C, Wu D, Zhang K, Khan FA, Pandupuspitasari NS, Wang Y, et al. 2022. Perfluorooctanoic acid alters the developmental trajectory of female germ cells and embryos in rodents and its potential mechanism. Ecotoxicol Environ Saf 236:113467, PMID: 35390687, https://doi.org/10.1016/j.ecoenv.2022.113467.
29. EFSA (European Food Safety Authority). 2008. Perfluorooctane sulfonate (PFOS), perfluorooctanic acid (PFOA) and their salts scientific opinion of the panel on contaminants in the food chain. EFSA J 6(7):653, PMID: 37213838, https://doi.org/10.2903/j.efsa.2008.653.
30. Lai KP, Lee JC, Wan HT, Li JW, Wong AY, Chan TF, et al. 2017. Effects of in utero PFOS exposure on transcriptome, lipidome, and function of mouse testis. Environ Sci Technol 51(15):8782–8794, PMID: 28654245, https://doi.org/10.1021/acs.est.7b02102.
31. Pertea M, Pertea GM, Antonescu CM, Chang TC, Mendell JT, Salzberg SL. 2015. StringTie enables improved reconstruction of a transcriptome from RNA-seq reads. Nat Biotechnol 33(3):290–295, PMID: 25690850, https://doi.org/10.1038/nbt.3122.

32. Love MI, Huber W, Anders S. 2014. Moderated estimation of fold change and dispersion for RNA-seq data with DESeq2. Genome Biol 15(12):550, PMID: 25516281, https://doi.org/10.1186/s13059-014-0550-8.

33. Klopfenstein DV, Zhang L, Pedersen BS, Ramírez F, Warwick Vesztrocy A, Naldi A, et al. 2018. GOATOOLS: a python library for gene ontology analyses. Sci Rep 8(1):10872, PMID: 30022098, https://doi.org/10.1038/s41598-018-28948-z.

34. Wu J, Mao X, Cai T, Luo J, Wei L. 2006. KOBAS server: a web-based platform for automated annotation and pathway identification. Nucleic Acids Res 34: W720–W724, PMID: 16845106, https://doi.org/10.1093/nar/gkl167.

35. Yu G, He QY. 2016. ReactomePA: an R/bioconductor package for reactome pathway analysis and visualization. Mol Biosyst 12(2):477–479, PMID: 26661513, https://doi.org/10.1039/c5mb00663e.

36. Subramanian A, Tamayo P, Mootha VK, Mukherjee S, Ebert BL, Gillette MA, et al. 2005. Gene set enrichment analysis: a knowledge-based approach for interpreting genome-wide expression profiles. Proc Natl Acad Sci USA 102(43):15545–15550, PMID: 16199517, https://doi.org/10.1073/pnas.0506580102.

37. Mootha VK, Lindgren CM, Eriksson KF, Subramanian A, Sihag S, Lehar J, et al. 2003. PGC-1alpha-responsive genes involved in oxidative phosphorylation are coordinately downregulated in human diabetes. Nat Genet 34(3):267–273, PMID: 12808457, https://doi.org/10.1038/ng1180.

38. Hänzelmann S, Castelo R, Guinney J. 2013. GSVA: gene set variation analysis for microarray and RNA-seq data. BMC Bioinformatics 14:7, PMID: 23323831, https://doi.org/10.1186/1471-2105-14-7.

39. Lv J, Li Y, Chen J, Li R, Bao C, Ding Z, et al. 2022. Maternal exposure to bis(2-ethylhexyl) phthalate during the thyroid hormone-dependent stage induces persistent emotional and cognitive impairment in middle-aged offspring mice. Food Chem Toxicol 163:112967, PMID: 35354077, https://doi.org/10.1016/j.fct.2022.112967.

40. Ouyang Y, Tong H, Luo P, Kong H, Xu Z, Yin P, et al. 2018. A high throughput metabolomics method and its application in female serum samples in a normal menstrual cycle based on liquid chromatography-mass spectrometry. Talanta 185:483–490, PMID: 29759231, https://doi.org/10.1016/j.talanta.2018.03.087.

41. UniProt Consortium. 2023. UniProt: the universal protein knowledgebase in 2023. Nucleic Acids Res 51(D1):D523–D531, PMID: 36408920, https://doi.org/10.1093/nar/gkac1052.

42. Kent WJ, Sugnet CW, Furey TS, Roskin KM, Pringle TH, Zahler AM, et al. 2002. The human genome browser at UCSC. Genome Res 12(6):996–1006, PMID: 12045153, https://doi.org/10.1101/gr.229102.

43. Robert X, Gouet P. 2014. Deciphering key features in protein structures with the new ENDscript server. Nucleic Acids Res 42:W320–W324, PMID: 24753421, https://doi.org/10.1093/nar/gku316.

44. Closs EI, Boissel JP, Habermeier A, Rotmann A. 2006. Structure and function of cationic amino acid transporters (CATs). J Membr Biol 213(2):67–77, PMID: 17417706, https://doi.org/10.1007/s00232-006-0875-7.

45. Kudo Y, Boyd CA. 2002. Human placental amino acid transporter genes: expression and function. Reproduction 124(5):593–600, PMID: 12416997, https://doi.org/10.1530/rep.0.1240593.

46. Jumper J, Evans R, Pritzel A, Green T, Figurnov M, Ronneberger O, et al. 2021. Highly accurate protein structure prediction with AlphaFold. Nature 596(7873):583–589, PMID: 34265844, https://doi.org/10.1038/s41586-021-03819-2.

47. Bangma J, Eaves LA, Oldenburg K, Reiner JL, Manuck T, Fry RC. 2020. Identifying risk factors for levels of per- and polyfluoroalkyl substances (PFAS) in the placenta in a high-risk pregnancy cohort in North Carolina. Environ Sci Technol 54(13):8158–8166, PMID: 32469207, https://doi.org/10.1021/acs.est.9b07102.

48. Kummu M, Sieppi E, Koponen J, Laatio L, Vähäkangas K, Kiviranta H, et al. 2015. Organic anion transporter 4 (OAT 4) modifies placental transfer of perfluorinated alkyl acids PFOS and PFOA in human placental ex vivo perfusion system. Placenta 36(10):1185–1191, PMID: 26303760, https://doi.org/10.1016/j.placenta.2015.07.119.

49. Li J, Cai D, Chu C, Li Q, Zhou Y, Hu L, et al. 2020. Transplacental transfer of per- and polyfluoroalkyl substances (PFASs): differences between preterm and full-term deliveries and associations with placental transporter mRNA expression. Environ Sci Technol 54(8):5062–5070, PMID: 32208722, https://doi.org/10.1021/acs.est.0c00829.

50. Szilagyi JT, Avula V, Fry RC. 2020. Perfluoroalkyl substances (PFAS) and their effects on the placenta, pregnancy, and child development: a potential mechanistic role for placental peroxisome proliferator-activated receptors (PPARs). Curr Environ Health Rep 7(3):222–230, PMID: 32812200, https://doi.org/10.1007/s40572-020-00279-0.

51. Blake BE, Cope HA, Hall SM, Keys RD, Mahler BW, McCord J, et al. 2020. Evaluation of maternal, embryo, and placental effects in CD-1 mice following gestational exposure to perfluorooctanoic acid (PFOA) or hexafluoropropylene oxide dimer acid (HFPO-DA or GenX). Environ Health Perspect 128(2):27006, PMID: 32074459, https://doi.org/10.1289/EHP6233.

52. Rinkenberger J, Werb Z. 2000. The labyrinthine placenta. Nat Genet 25(3):248–250, PMID: 10888863, https://doi.org/10.1038/76985.

53. Jaiman S, Romero R, Pacora P, Jung E, Bhatti G, Yeo L, et al. 2020. Disorders of placental villous maturation in fetal death. J Perinat Med, PMID: 32238609, https://doi.org/10.1515/jpm-2020-0030.

54. Wang Z, Gerstein M, Snyder M. 2009. RNA-Seq: a revolutionary tool for transcriptomics. Nat Rev Genet 10(1):57–63, PMID: 19015660, https://doi.org/10.1038/nrg2484.

55. Wheeler MA, Jaronen M, Covacu R, Zandee SEJ, Scalisi G, Rothhammer V, et al. 2019. Environmental control of astrocyte pathogenic activities in CNS inflammation. Cell 176(3):581–596, PMID: 30661753, https://doi.org/10.1016/j.cell.2018.12.012.

56. Mayeur S, Lancel S, Theys N, Lukaszewski MA, Duban-Deweer S, Bastide B, et al. 2013. Maternal calorie restriction modulates placental mitochondrial biogenesis and bioenergetic efficiency: putative involvement in fetoplacental growth defects in rats. Am J Physiol Endocrinol Metab 304(1):E14–E22, PMID: 23092912, https://doi.org/10.1152/ajpendo.00332.2012.

57. Chae SA, Son JS, Du M. 2022. Prenatal exercise in fetal development: a placental perspective. FEBS J 289(11):3058–3071, PMID: 34449982, https://doi.org/10.1111/febs.16173.

58. Taggi V, Riera Romo M, Piquette-Miller M, Meyer Zu Schwabedissen HE, Neuhoff S. 2022. Transporter regulation in critical protective barriers: focus on brain and placenta. Pharmaceutics 14(7):1376, PMID: 35890272, https://doi.org/10.3390/pharmaceutics14071376.

59. Lin L, Yee SW, Kim RB, Giacomini KM. 2015. SLC transporters as therapeutic targets: emerging opportunities. Nat Rev Drug Discov 14(8):543–560, PMID: 26111766, https://doi.org/10.1038/nrd4626.

60. Cooper TA, Wan L, Dreyfuss G. 2009. RNA and disease. Cell 136(4):777–793, PMID: 19239895, https://doi.org/10.1016/j.cell.2009.02.011.

61. Calkhoven CF, Müller C, Leutz A. 2002. Translational control of gene expression and disease. Trends Mol Med 8(12):577–583, PMID: 12470991, https://doi.org/10.1016/s1471-4914(02)02424-3.

62. Lee TI, Young RA. 2013. Transcriptional regulation and its misregulation in disease. Cell 152(6):1237–1251, PMID: 23498934, https://doi.org/10.1016/j.cell.2013.02.014.

63. Sonawane AR, Platig J, Fagny M, Chen C-Y, Paulson JN, Lopes-Ramos CM, et al. 2017. Understanding tissue-specific gene regulation. Cell Rep 21(4):1077–1088, PMID: 29069589, https://doi.org/10.1016/j.celrep.2017.10.001.

64. Buccitelli C, Selbach M. 2020. mRNAs, proteins and the emerging principles of gene expression control. Nat Rev Genet 21(10):630–644, PMID: 32709985, https://doi.org/10.1038/s41576-020-0258-4.

65. Wright CJ, Smith CWJ, Jiggins CD. 2022. Alternative splicing as a source of phenotypic diversity. Nat Rev Genet 23(11):697–710, PMID: 35821097, https://doi.org/10.1038/s41576-022-00514-4.

66. Marasco LE, Kornblihtt AR. 2023. The physiology of alternative splicing. Nat Rev Mol Cell Biol 24(4):242–254, PMID: 36229538, https://doi.org/10.1038/s41580-022-00545-z.

67. Ule J, Blencowe BJ. 2019. Alternative splicing regulatory networks: functions, mechanisms, and evolution. Mol Cell 76(2):329–345, PMID: 31626751, https://doi.org/10.1016/j.molcel.2019.09.017.

68. Tan C, Huang Z, Xiong W, Ye H, Deng J, Yin Y. 2022. A review of the amino acid metabolism in placental function response to fetal loss and low birth weight in pigs. J Anim Sci Biotechnol 13(1):28, PMID: 35232472, https://doi.org/10.1186/s40104-022-00676-5.

69. Xu L, Wang X, Wang C, Li W, Liu H. 2022. L-arginine supplementation improved neonatal outcomes in pregnancies with hypertensive disorder or intrauterine growth restriction: a systematic review and meta-analysis of randomized controlled trials. Clin Nutr 41(7):1512–1522, PMID: 35667267, https://doi.org/10.1016/j.clnu.2022.05.014.

70. Punshon T, Li Z, Jackson BP, Parks WT, Romano M, Conway D, et al. 2019. Placental metal concentrations in relation to placental growth, efficiency and birth weight. Environ Int 126:533–542, PMID: 30851484, https://doi.org/10.1016/j.envint.2019.01.063.

71. Deyssenroth MA, Gennings C, Liu SH, Peng S, Hao K, Lambertini L, et al. 2018. Intrauterine multi-metal exposure is associated with reduced fetal growth through modulation of the placental gene network. Environ Int 120:373–381, PMID: 30125854, https://doi.org/10.1016/j.envint.2018.08.010.

72. Li R, Wang X, Wang B, Li J, Song Y, Luo B, et al. 2018. Gestational 1-nitropyrene exposure causes fetal growth restriction through disturbing placental vascularity and proliferation. Chemosphere 213:252–258, PMID: 30223130, https://doi.org/10.1016/j.chemosphere.2018.09.059.

73. Kurosaki T, Popp MW, Maquat LE. 2019. Quality and quantity control of gene expression by nonsense-mediated mRNA decay. Nat Rev Mol Cell Biol 20(7):406–420, PMID: 30992545, https://doi.org/10.1038/s41580-019-0126-2.

74. Garber M, Grabherr MG, Guttman M, Trapnell C. 2011. Computational methods for transcriptome annotation and quantification using RNA-seq. Nat Methods 8(6):469–477, PMID: 21623353, https://doi.org/10.1038/nmeth.1613.

75. Chen M, Manley JL. 2009. Mechanisms of alternative splicing regulation: insights from molecular and genomics approaches. Nat Rev Mol Cell Biol 10(11):741–754, PMID: 19773805, https://doi.org/10.1038/nrm2777.

76. Sun J, Fang R, Wang H, Xu DX, Yang J, Huang X, et al. 2022. A review of environmental metabolism disrupting chemicals and effect biomarkers associating disease risks: where exposomics meets metabolomics. Environ Int 158:106941, PMID: 34689039, https://doi.org/10.1016/j.envint.2021.106941.

77. Li X, Ye L, Ge Y, Yuan K, Zhang Y, Liang Y, et al. 2016. In utero perfluorooctane sulfonate exposure causes low body weights of fetal rats: a mechanism study. Placenta 39:125–133, PMID: 26992685, https://doi.org/10.1016/j.placenta.2016.01.010.